

INTEGRABILITY AND COMBINATORICS: SELECTED TOPICS

PAUL ZINN-JUSTIN

ABSTRACT. These are notes for Les Houches July 2008.

CONTENTS

Introduction	1
1. Free fermionic methods	2
1.1. Definitions	2
1.2. Schur functions	5
1.3. From free fermions to Schur functions	6
1.4. Application: Plane Partition enumeration	12
1.5. Classical integrability	16
2. The six-vertex model	16
2.1. Definition	16
2.2. Integrability	18
2.3. Phase diagram	19
2.4. Equivalence to loop models	21
2.5. Domain Wall Boundary Conditions	22
3. Razumov–Stroganov conjecture	26
3.1. Some boundary observables for loop models	26
3.2. Properties of the steady state	29
3.3. The quantum Knizhnik–Zamolodchikov equation	32
References	38

INTRODUCTION

The purpose of these lectures is twofold. On the one hand, they will try to show how methods coming from modern physics and more specifically from quantum integrable models can be used to solve difficult problems of enumerative combinatorics. As the field of combinatorics is expanding rapidly, problems of enumeration become more and more difficult and direct combinatorial proofs often become extremely complicated and tedious. This is where physical ideas can come in to provide conceptually simple proofs. On the other hand, these

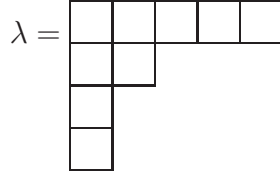
Date: January 16, 2009.

PZJ is supported by EU Marie Curie Research Training Networks “ENRAGE” MRTN-CT-2004-005616, “ENIGMA” MRT-CT-2004-5652, ESF program “MISGAM” and ANR program “GIMP” ANR-05-BLAN-0029-01.

which will be useful in what follows. They satisfy

$$(5) \quad \psi_k |\ell\rangle = 0 \quad k > \ell, \quad \psi_k^* |\ell\rangle = 0 \quad k < \ell$$

More generally, define a *partition* to be a weakly decreasing finite sequence of non-negative integers: $\lambda_1 \geq \lambda_2 \geq \dots \geq \lambda_n \geq 0$. We usually represent partitions as *Young diagrams*: for example $\lambda = (5, 2, 1, 1)$ is depicted as

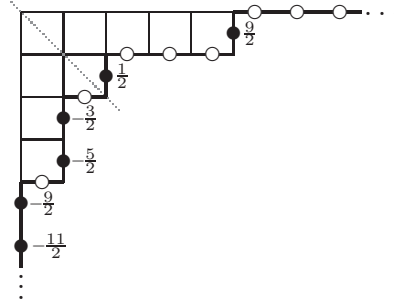


To each partition $\lambda = (\lambda_1, \dots, \lambda_n)$ we associate the following state in \mathcal{F}_ℓ :

$$(6) \quad |\lambda; \ell\rangle = \psi_{\ell+\lambda_1-\frac{1}{2}}^* \psi_{\ell+\lambda_2-\frac{3}{2}}^* \cdots \psi_{\ell+\lambda_n-n+\frac{1}{2}}^* |\ell - n\rangle$$

Note the important property that if one “pads” a partition with extra zeroes, then the corresponding state remains unchanged. In particular for the empty diagram \emptyset , $|\emptyset; \ell\rangle = |\ell\rangle$. For $\ell = 0$ we just write $|\lambda; 0\rangle = |\lambda\rangle$.

This definition has the following nice graphical interpretation: the state $|\lambda; \ell\rangle$ can be described by numbering the edges of the boundary of the Young diagram, in such a way that the main diagonal passes between $\ell - \frac{1}{2}$ and $\ell + \frac{1}{2}$; then the occupied (resp. empty) sites correspond to vertical (resp. horizontal) edges. With the example above and $\ell = 0$, we find (only the occupied sites are numbered for clarity)



Finally, introduce the normal ordering with respect to the vacuum $|0\rangle$:

$$(8) \quad :\psi_j^* \psi_k: = -:\psi_k \psi_j^*: = \begin{cases} \psi_j^* \psi_k & j > 0 \\ -\psi_k \psi_j^* & j < 0 \end{cases}$$

which allows to get rid of trivial infinite quantities.

1.1.2. *The relativistic chiral fermion.* One possible interpretation of these operators is that they correspond to chiral massless relativistic charged free fermions, with (1) solving implicitly the equations of motion. Indeed if z is a complex variable which represents space-time, then ψ and ψ^* satisfy $\bar{\partial}\psi(z) = \bar{\partial}\psi^*(z) = 0$, which is the solution of the equations of motion for a free fermion with action $S = \int d^2z \psi^*(z) \bar{\partial}\psi(z)$, or with Hamiltonian $H = \sum_k k : \psi_k^* \psi_k :$.

This is not the point of view we shall adopt in the rest of these lectures, since the dynamics of our system will be given by a different type of Hamiltonian (though it will be quadratic, resulting in a free theory as well). In fact, it is more natural to think of the k as being position, and therefore of z as momentum (with $|z| = 1$), though this is to some extent a matter of taste.

Note for example that one can derive the following formula using solely the construction of the previous section (the proof is elementary and left to the reader – careful with the signs!)

$$(9) \quad \langle \ell | \psi(w_r) \cdots \psi(w_1) \psi^*(z_1) \cdots \psi^*(z_s) | m \rangle \\ = \delta_{\ell+r, m+s} \prod_{i=1}^r w_i^{-m} \prod_{j=1}^s z_j^m \frac{\prod_{1 \leq i < j \leq r} (w_j - w_i) \prod_{1 \leq i < j \leq s} (z_i - z_j)}{\prod_{1 \leq i \leq r, 1 \leq j \leq s} (w_i - z_j)}$$

But this is in fact the Wick theorem for free fermions with propagator $\langle \psi(w) \psi^*(z) \rangle = \frac{1}{w-z}$.

1.1.3. *$\mathfrak{gl}(\infty)$ and $\hat{\mathfrak{u}}(1)$ action.* The bilinears $\psi^*(z)\psi(w)$ give rise to the Schwinger representation of $\mathfrak{gl}(\infty)$ on \mathcal{F} , whose usual basis is the $:\psi_r^* \psi_s:$, $r, s \in \mathbb{Z} + \frac{1}{2}$, and the identity. In the first quantized picture this representation is simply the natural action of $\mathfrak{gl}(\infty)$ on the one-particle Hilbert space $\mathbb{C}^{\mathbb{Z} + \frac{1}{2}}$ and exterior products thereof. The electric charge $J_0 = \sum_r :\psi_r^* \psi_r:$ is a conserved number and classifies the irreducible representations of $\mathfrak{gl}(\infty)$ inside \mathcal{F} , which are all isomorphic. The highest weight vectors are precisely our vacua $|\ell\rangle$, $\ell \in \mathbb{Z}$, so that $\mathcal{F} = \bigoplus_{\ell \in \mathbb{Z}} \mathcal{F}_\ell$ with \mathcal{F}_ℓ the subspace in which $J_0 = \ell$.

The $\mathfrak{u}(1)$ current

$$(10) \quad j(z) = :\psi^*(z)\psi(z): = \sum_{n \in \mathbb{Z}} J_n z^{-n-1}$$

with $J_n = \sum_r :\psi_{r-n}^* \psi_r:$ forms a $\hat{\mathfrak{u}}(1)$ (Heisenberg) subalgebra of $\mathfrak{gl}(\infty)$:

$$(11) \quad [J_m, J_n] = m \delta_{m, -n}$$

Note in particular that positive modes commute among themselves. This allows to define the general ‘‘Hamiltonian’’

$$(12) \quad H[t] = \sum_{q=1}^{\infty} t_q J_q$$

where $t = (t_1, \dots, t_q, \dots)$ is a set of parameters (‘‘times’’).

The J_q , $q > 0$, displace one of the fermions q steps to the left. This is expressed by the formulae describing the time evolution of the fermionic fields:

$$(13) \quad \begin{aligned} e^{H[t]}\psi(z)e^{-H[t]} &= e^{-\sum_{q=1}^{\infty} t_q z^q} \psi(z) \\ e^{H[t]}\psi^*(z)e^{-H[t]} &= e^{+\sum_{q=1}^{\infty} t_q z^q} \psi^*(z) \end{aligned}$$

(proof: compute $[J_q, \psi^{[*]}(z)] = \pm z^q \psi^{[*]}(z)$ and exponentiate). Of course, similarly, J_{-q} , $q > 0$, moves one fermion q steps to the right.

1.2. Schur functions. Schur functions are undoubtedly the most important basis in the theory of symmetric functions (symmetric polynomials of an arbitrarily large number of variables). As we shall see, they are also closely connected to free fermions.

1.2.1. Definition. There are several ways to define Schur functions. We use the following. Let λ be a partition. Then the associated Schur function s_λ is

$$(14) \quad s_\lambda(x_1, \dots, x_n) = \frac{\det_{1 \leq i, j \leq n} (x_i^{\lambda_j + n - j})}{\prod_{i < j} (x_i - x_j)}$$

This is sometimes called the Weyl formula. Here it is assumed that λ has been padded to the number of variables. If there are fewer variables than the number of non-zero parts of λ , then $s_\lambda = 0$. Note that the denominator is nothing but the numerator for $\lambda_j = 0$ (up to a sign it is the Vandermonde determinant), so that $s_\emptyset = 1$. One can think of numerator/denominator as the (Slater) wave function of n fermions in a first quantized picture, the numerator being an excited state and the denominator being the ground state. The connection between Schur functions and free fermions that we shall establish later is essentially a refined, second quantized version of this idea.

$s_\lambda(x_1, \dots, x_n)$ is explicitly symmetric by permutation of its arguments. It is also not too hard to check that $s_\lambda(x_1, \dots, x_n, 0, \dots, 0) = s_\lambda(x_1, \dots, x_n)$, that is s_λ satisfies a stability property with respect to the number of variables.

Since the numerator vanishes when any two x_i coincide, the denominator divides the numerator, so that s_λ is a polynomial of the x_i . In fact one can easily see that it is a homogeneous polynomial of degree the number of boxes of λ .

Remark: defined in terms of a fixed number n of variables, as in (14), $s_\lambda(x_1, \dots, x_n)$ has the following group-theoretic interpretation. The polynomial irreducible representations of $GL(n)$ are known to be indexed by partitions. More precisely, the representation on tensors of order k decomposes as a direct sum of isotypic representations corresponding to every partition λ such that $|\lambda| = k$. Then $s_\lambda(x_1, \dots, x_n)$ is the character of representation λ evaluated at the diagonal matrix $\text{diag}(x_1, \dots, x_n)$. Hence, the dimension of λ as a $GL(n)$ representation is given by $s_\lambda(\underbrace{1, \dots, 1}_n) = \prod_{1 \leq i < j \leq n} (\lambda_i - i - \lambda_j + j) / (j - i)$. (proof: use $x_i = q^i$,

compute and send q to 1)

$$\text{Examples: } s_{\square} = \sum_i x_i, \quad s_{\begin{smallmatrix} \square \\ \square \end{smallmatrix}} = \sum_{i < j} x_i x_j, \quad s_{\begin{smallmatrix} \square & \square \\ \square & \square \end{smallmatrix}} = \sum_{i \leq j} x_i x_j.$$

1.2.2. Power sums. Any symmetric polynomial of some variables x_i is in fact a polynomial of its power sums, i.e.

$$t_q = \frac{1}{q} \sum_i x_i^q \quad q \geq 1$$

If there are n variables, only n of the t_q are independent; however for symmetric functions (i.e. for an arbitrarily large number of variables) they should be considered as independent.

We shall often use this parameterization for Schur functions; we denote it $s_\lambda[t_1, \dots, t_q, \dots]$ or simply $s_\lambda[t]$.

Note that transposition of diagram corresponds to changing the sign of even power sums:

$$s_{\lambda'}[t_1, t_2, \dots, t_q, \dots] = s_\lambda[t_1, -t_2, \dots, (-1)^{q-1}t_q, \dots]$$

Examples: $s_{\square} = t_1$, $s_{\begin{smallmatrix} \square \\ \square \end{smallmatrix}} = \frac{1}{2}t_1^2 - t_2$, $s_{\begin{smallmatrix} \square & \square \\ \square & \square \end{smallmatrix}} = \frac{1}{2}t_1^2 + t_2$, $s_{\begin{smallmatrix} \square & \square & \square \\ \square & \square & \square \end{smallmatrix}} = \frac{1}{3}t_1^3 - t_3$.

Remark: According to Schur–Weyl duality, the coefficients of the expansion of s_λ in products of t 's are known (Frobenius formula): they are essentially characters of the symmetric group. As a corollary, the dimension of λ as a representation of the symmetric group is given by $|\lambda|! s_\lambda[1, 0, \dots, 0, \dots]$.

1.3. From free fermions to Schur functions.

1.3.1. *Basic relation.* We now prove the following important identity:

$$(15) \quad \langle \ell | e^{H[t]} | \lambda; \ell \rangle = s_\lambda[t]$$

which shows that the map $|\Phi\rangle \mapsto \langle \ell | e^{H[t]} |\Phi\rangle$ is an isomorphism from \mathcal{F}_ℓ to the space of symmetric functions.

Proof. Due to obvious translational invariance of all the operators involved, we may as well set $\ell = n$. Use the definition (6) of $|\lambda\rangle$ and the commutation relations (13) to rewrite the left hand side as

$$\langle n | e^{H[t]} | \lambda; n \rangle = e^{\sum_{q \geq 1} t_q \sum_{i=1}^n z_i^q} \langle n | \psi^*(z_1) \psi^*(z_2) \cdots \psi^*(z_n) | 0 \rangle \Big|_{z_1^{n+\lambda_1-1} z_2^{n+\lambda_2-2} \cdots z_n^{\lambda_n}}$$

where $| \dots \rangle$ means picking one term in a generating series.

As a special case of (9), we can evaluate the remaining bra-ket to be: (we now use the $\ell = 0$ notation for the l.h.s.)

$$\langle 0 | e^{H[t]} | \lambda \rangle = e^{\sum_{q \geq 1} t_q \sum_{i=1}^n z_i^q} \prod_{1 \leq i < j \leq n} (z_i - z_j) \Big|_{z_1^{n+\lambda_1-1} z_2^{n+\lambda_2-2} \cdots z_n^{\lambda_n}}$$

Now write $t_q = \frac{1}{q} \sum_{j=1}^n x_j^q$ and note that $e^{\sum_{q \geq 1} t_q \sum_{i=1}^n z_i^q} = \prod_{i,j=1}^n (1 - z_i x_j)^{-1}$. We recognize (part of) the Cauchy determinant:

$$\langle 0 | e^{H[t]} | \lambda \rangle = \frac{\det_{1 \leq i, j \leq n} (1 - x_i z_j)^{-1}}{\prod_{i < j} (x_i - x_j)} \Big|_{z_1^{n+\lambda_1-1} z_2^{n+\lambda_2-2} \cdots z_n^{\lambda_n}}$$

At this stage we can just expand separately each column of the matrix $(1 - x_i z_j)^{-1}$ to pick the right power of z_j ; we find:

$$\langle 0 | e^{H[t]} | \lambda \rangle = \frac{\det_{1 \leq i, j \leq n} (x_i^{\lambda_j + n - j})}{\prod_{i < j} (x_i - x_j)}$$

which is our definition (14) of a Schur function. □

We shall now compute in various ways $\langle 0 | e^{H[t]} | \lambda \rangle$. In fact, many of the methods used are equally applicable to the following more general quantity:

$$(16) \quad s_{\lambda/\mu}[t] = \langle \mu | e^{H[t]} | \lambda \rangle$$

where λ and μ are two partitions. It is easy to see that in order for $s_{\lambda/\mu}[t]$ to be non-zero, $\mu \subset \lambda$ as Young diagrams; in this case $s_{\lambda/\mu}$ is known as the *skew Schur function* associated to the skew Young diagram λ/μ . The latter is depicted as the complement of μ inside λ . This is appropriate because skew Schur functions factorize in terms of the connected components of the skew Young diagram λ/μ .

$$\text{Examples: } s_{\begin{array}{|c|} \hline \square \\ \hline \end{array}} = s_{\begin{array}{|c|} \hline \square \\ \hline \end{array}}^2 = t_1^2, \quad s_{\begin{array}{|c|c|} \hline \square & \square \\ \hline \end{array}} = \frac{5}{24}t_1^4 + \frac{1}{2}t_1^2t_2 + \frac{1}{2}t_2^2 - t_1t_3 - t_4.$$

1.3.2. *Wick theorem and Jacobi–Trudi identity.* First, we apply the Wick theorem. Consider as the definition of the time evolution of fermionic fields:

$$(17) \quad \begin{aligned} \psi_k[t] &= e^{H[t]} \psi_k e^{-H[t]} \\ \psi_k^*[t] &= e^{H[t]} \psi_k^* e^{-H[t]} \end{aligned}$$

In fact, (13) gives us the “solution” of the equations of motion in terms of the generating series $\psi(z)$, $\psi^*(z)$.

Noting that the Hamiltonian is quadratic in the fields, we now state the Wick theorem:

$$(18) \quad \langle \ell | \psi_{i_1}[0] \cdots \psi_{i_n}[0] \psi_{j_1}^*[t] \cdots \psi_{j_n}^*[t] | \ell \rangle = \det_{1 \leq p, q \leq n} \langle \ell | \psi_{i_p}[0] \psi_{j_q}^*[t] | \ell \rangle$$

Next, start from the expression (16) of $s_{\lambda/\mu}[t]$: padding with zeroes λ or μ so that they have the same number of parts n , we can write

$$s_{\lambda/\mu}[t] = \langle -n | \psi_{\mu_n - n + \frac{1}{2}} \cdots \psi_{\mu_1 - \frac{1}{2}} e^{H[t]} \psi_{\lambda_1 - \frac{1}{2}}^* \cdots \psi_{\lambda_n - n + \frac{1}{2}}^* | -n \rangle$$

and apply the Wick theorem to find:

$$s_{\lambda/\mu}[t] = \det_{1 \leq p, q \leq n} \langle -n | \psi_{\mu_p - p + \frac{1}{2}} e^{H[t]} \psi_{\lambda_q - q + \frac{1}{2}}^* | -n \rangle$$

It is easy to see that $\langle -n | \psi_i e^{H[t]} \psi_j^* | -n \rangle$ does not depend on n and thus only depends on $j - i$. Let us denote it

$$(19) \quad h_k[t] = \langle 1 | e^{H[t]} \psi_{k+\frac{1}{2}}^* | 0 \rangle \quad \sum_{k \geq 0} h_k[t] z^k = \langle 1 | e^{H[t]} \psi^*(z) | 0 \rangle = e^{\sum_{q \geq 1} t_q z^q}$$

($k = j - i$; note that $h_k[t] = 0$ for $k < 0$).

The final formula we obtain is

$$(20) \quad s_{\lambda/\mu}[t] = \det_{1 \leq p, q \leq n} (h_{\lambda_q - \mu_p - q + p}[t])$$

or, for regular Schur functions,

$$(21) \quad s_\lambda[t] = \det_{1 \leq p, q \leq n} (h_{\lambda_q - q + p}[t])$$

This is known as the Jacobi–Trudi identity.

By using “particle–hole duality”, we can find a dual form of this identity. We describe our states in terms of hole positions, parameterized by the lengths of the columns λ'_p and μ'_q , according to (7):

$$s_{\lambda/\mu}[t] = (-1)^{|\lambda|+|\mu|} \langle m | \psi_{-\mu'_m+m-\frac{1}{2}}^* \cdots \psi_{-\mu'_1+\frac{1}{2}}^* e^{H[t]} \psi_{-\lambda'_1+\frac{1}{2}} \cdots \psi_{-\lambda'_m+m-\frac{1}{2}} | m \rangle$$

Again the Wick theorem applies and expresses $s_{\lambda/\mu}$ in terms of the two point-function $\langle m | \psi_i^* e^{H[t]} \psi_j | m \rangle$, which only depends on $i - j = k$ and is given by (22)

$$e_k[t] = (-1)^k \langle -1 | e^{H[t]} \psi_{-k+\frac{1}{2}} | 0 \rangle \quad \sum_{k \geq 0} e_k[t] z^k = \langle -1 | e^{H[t]} \psi(-z) | 0 \rangle = e^{\sum_{q \geq 1} (-1)^{q-1} t_q z^q}$$

The finally formula takes the form

$$(23) \quad s_{\lambda/\mu}[t] = \det_{1 \leq p, q \leq n} (e_{\lambda'_q - \mu'_p - q + p}[t])$$

or, for regular Schur functions,

$$(24) \quad s_\lambda[t] = \det_{1 \leq p, q \leq n} (e_{\lambda'_q - q + p}[t])$$

This is the dual Jacobi–Trudi identity, also known as Von Nögelsbach–Kostka identity.

1.3.3. *Schur functions and lattice fermions.* In the following three sections 1.3.3–1.3.5, we shall assume a fixed, finite number of variables n , and set as before $t_q = \frac{1}{q} \sum_{i=1}^n x_i^q$. In this case we can write

$$e^{H[t]} = \prod_{i=1}^n e^{\phi_+(x_i)} \quad \phi_+(x) = \sum_{q \geq 1} \frac{x^q}{q} J_q$$

So we can think of the “time evolution” as a series of discrete steps represented by commuting operators $\exp \phi_+(x_i)$. In the language of statistical mechanics, these are transfer matrices (and the one-parameter family of transfer matrices $\exp \phi_+(x)$ is of course related to the integrability of the model). We now show that they have a very simple meaning in terms of lattice fermions.

Consider a two-dimensional square lattice, one direction being our space $\mathbb{Z} + \frac{1}{2}$ and one direction being time. In what follows we shall reverse the arrow of time (that is, we shall consider that time flows upwards on the pictures), which makes the discussion slightly easier since products of operators are read from left to right. The rule to go from one step to the next according to the evolution operator $\exp \phi_+(x)$ can be formulated either in terms of particles or in terms of holes:

- Each particle can go straight or hop to the right as long as it does not reach the (original) location of the next particle. Each step to the right is given a weight of x .
- Each hole can only go straight or one step to the left as long as it does not bump into its neighbor. Each step to the left is given a weight of x .

Obviously the second description is simpler. An example of a possible evolution of the system with given initial and final states is shown on Fig. 1(a).

The proof of these rules consists in computing explicitly $\langle \mu | e^{\phi_+(x)} | \lambda \rangle$ by applying say (23) for $t_q = \frac{1}{q} x^q$, and noting that in this case, according to (22), $e_n[t] = 0$ for $n > 1$. This strongly constrains the possible transitions and produces the description above.

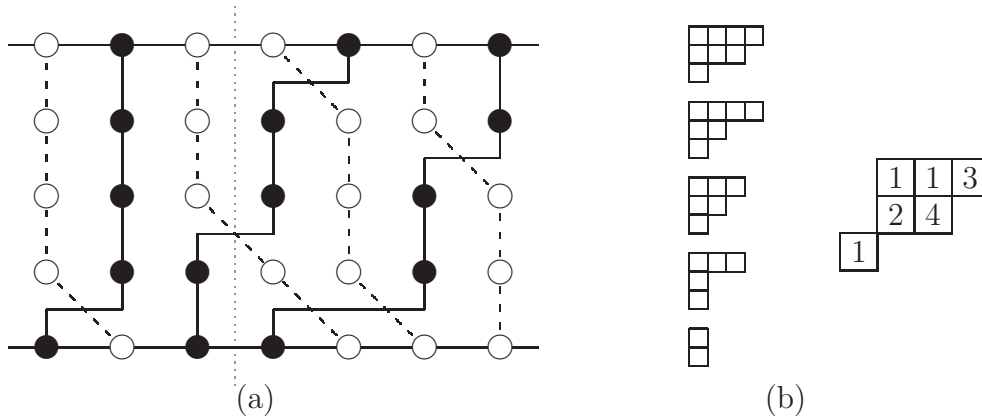


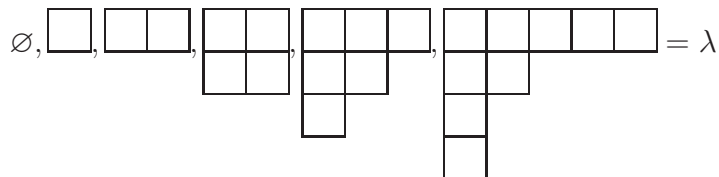
FIGURE 1. A lattice fermion configuration and the corresponding (skew) SSYT.

1.3.4. *Relation to Semi-Standard Young tableaux.* A semi-standard Young tableau (SSYT) of shape λ is a filling of the Young diagram of λ with elements of some ordered alphabet, in such a way that rows are weakly increasing and columns are strictly increasing.

We shall use here the alphabet $\{1, 2, \dots, n\}$. For example with $\lambda = (5, 2, 1, 1)$ one possible SSYT with $n \geq 5$ is:

1	2	4	5	5
3	3			
4				
5				

It is useful to think of Young tableaux as time-dependent Young diagrams where the number indicates the step at which a given box was created. Thus, with the same example, we get



In other words, a Young tableau is nothing but a statistical configuration of our lattice fermions, where the initial state is the vacuum. Similarly, a skew SSYT is a filling of a skew Young diagram with the same rules; it corresponds to a statistical configuration of lattice fermions with arbitrary initial and final states. The correspondence is exemplified on Fig. 1(b).

Each extra box corresponds to a step to the right for particles or to the left for holes. The initial and final states are \emptyset and λ , which is the case for Schur functions, cf (15). We conclude that the following formula holds:

$$(25) \quad s_\lambda(x_1, \dots, x_n) = \sum_{T \in \text{SSYT}(\lambda, n)} \prod_{b \text{ box of } T} x_{T_b}$$

This is often taken as a definition of Schur functions. It is explicitly stable with respect to n in the sense that $s_\lambda(x_1, \dots, x_n, 0, \dots, 0) = s_\lambda(x_1, \dots, x_n)$. It is however not obvious from it that s_λ is symmetric by permutation of its variables. This fact is a manifestation of the underlying free fermionic (“integrable”) behavior. Of course an identical formula holds for the more general case of skew symmetric Schur functions.

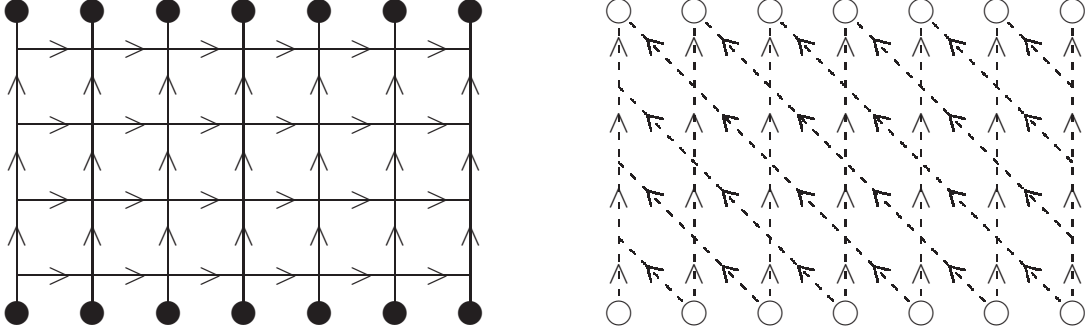


FIGURE 2. Underlying directed graphs for particles and holes.

1.3.5. *Non-Intersecting Lattice Paths and Lindström–Gessel–Viennot formula.* The rules of evolution given in section 1.3.3 strongly suggest the following explicit description of the lattice fermion configurations. Consider the directed graphs of Fig. 2 (the graphs are in principle infinite to the left and right, but any given bra-ket evaluation only involves a finite number of particles and holes and therefore the graphs can be truncated to a finite part). Consider *Non-Intersecting Lattice Paths* (NILPs) on these graphs: they are paths with given starting points (at the bottom) and given ending points (at the top), which follow the edges of the graph respecting the orientation of the arrows, and which are not allowed to touch at any vertices. One can check that the trajectories of holes and particles following the rules described in section 1.3.3 are exactly the most general NILPs on these graphs.

In this context, the Wick theorem (21) (i.e. the Jacobi–Trudi identity) is most naturally proved in the “functional integral” formalism. We recall it here.

Assign to each vertex of the graph Grassmann variables χ_i and χ_i^* and consider the action

$$-S = \sum_i \chi_i \chi_i^* + \sum_{i \rightarrow j} w_{ij} \chi_i^* \chi_j$$

where the w_{ij} are arbitrary weights on the directed edges $i \rightarrow j$. Then one has the following identity: the weighted sum of paths from starting locations i_1, \dots, i_n to ending locations j_1, \dots, j_n , where the weight of a path is the products of weights of the edges, is given by

$$N(i_1, \dots, i_n; j_1, \dots, j_n) = \langle \chi_{i_1}^* \cdots \chi_{i_n}^* \chi_{j_n} \cdots \chi_{j_1} \rangle$$

In this formula, averaging is with respect to the measure $\exp(-S)$. The Wick theorem for Gaussian integrals then asserts that $\langle \chi_{i_1}^* \cdots \chi_{i_n}^* \chi_{j_n} \cdots \chi_{j_1} \rangle = \det_{p,q} \langle \chi_{i_p}^* \chi_{j_q} \rangle$, or

$$(26) \quad N(i_1, \dots, i_n; j_1, \dots, j_n) = \det_{p,q} N(i_p; j_q)$$

This result is clearly valid for any planar directed acyclic graph (and with appropriate starting/endpoints: no paths between starting points or between endpoints should be possible). In combinatorics, the formula (26) is known as the Lindström–Gessel–Viennot formula [2, 7].

So we only need to compute $N(i; j)$, the weighted number of paths from i to j . Let us do so in our problem.

In the case of particles (left graph), numbering the initial and final points from left to right, we find that the weighted sum of paths from i to j , where a weight x_i is given to each right move at timestep i , only depends on $j - i$; if we denote it by $h_{j-i}(x_1, \dots, x_n)$, we have

the obvious generating series formula

$$\sum_{k \geq 0} h_k(x_1, \dots, x_n) z^k = \prod_{i=1}^n \frac{1}{1 - zx_i}$$

Note that this formula coincides with the alternate definition (19) of $h_k[t]$ if we set as usual $t_q = \frac{1}{q} \sum_{i=1}^n x_i^q$. Thus, applying the LGV formula (26) and choosing the correct initial and final points for Schur functions or skew Schur functions, we recover immediately (20,21).

In the case of holes (right graph), numbering the initial and final points from right to left, we find once again that the weighted sum of paths from i to j , where a weight x_i is given to each left move at timestep i , only depends on $j - i$; if we denote it by $e_{j-i}(x_1, \dots, x_n)$, we have the equally obvious generating series formula

$$\sum_{k \geq 0} e_k(x_1, \dots, x_n) z^k = \prod_{i=1}^n (1 + zx_i)$$

which coincides with (22), thus allowing us to recover (23,24).

1.3.6. *Relation to Standard Young Tableaux.* A Standard Young Tableau (SYT) of shape λ is a filling of the Young diagram of λ with elements of some ordered alphabet, in such a way that both rows and columns are strictly increasing. There is no loss of generality in assuming that the alphabet is $\{1, \dots, n\}$, where $n = |\lambda|$ is the number of boxes of λ . For example,

1	2	6	8	9
3	4			
5				
7				

is a SYT of shape $(5, 2, 1, 1)$.

Standard Young Tableaux are connected to the representation theory of the symmetric group; in particular the number of such tableaux with given shape λ is the dimension of λ as an irreducible representation of the symmetric group, which is up to a trivial factor the evaluation of the Schur function s_λ at $t_q = \delta_{1q}$. In this case one has $H[t] = J_1$, and there is only one term contributing to the bra-ket $\langle \lambda | e^{H[t]} | 0 \rangle$ in the expansion of the exponential:

$$s_\lambda[\delta_{1.}] = \frac{1}{n!} \langle \lambda | J_1^n | 0 \rangle$$

In terms of lattice fermions, J_1 has a direct interpretation as the transfer matrix for one particle hopping one step to the left. As the notion of SYT is invariant by transposition, particles and holes play a symmetric role so that the evolution can be summarized by either of the two rules:

- Exactly one particle moves one step to the right in such a way that it does not bump into its neighbor; all the other particles go straight.
- Exactly one hole moves one step to the left in such a way that it does not bump into its neighbor; all the other holes go straight.

An example of such a configuration is given on Fig. 3.

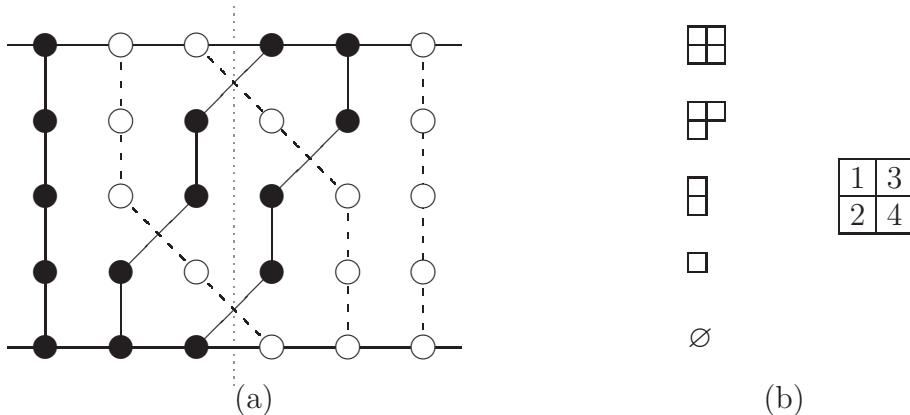


FIGURE 3. A lattice fermion configuration and the corresponding SYT.

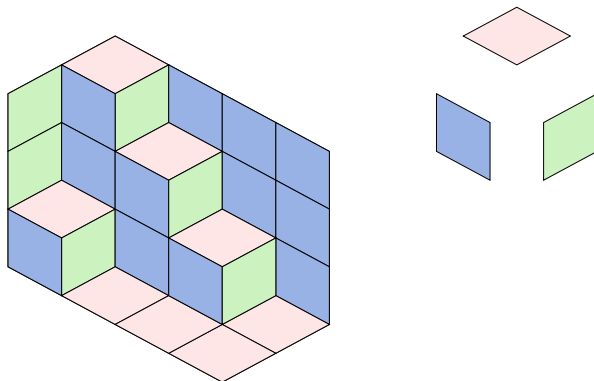


FIGURE 4. A plane partition of size $2 \times 3 \times 4$.

1.4. Application: Plane Partition enumeration. *Plane partitions* are an important class of objects in combinatorics. The name originates from the way they were first introduced [1] as two-dimensional generalizations of partitions. Here we shall directly define them graphically.

1.4.1. *Definition.* Intuitively, plane partitions are pilings of boxes (cubes) in the corner of a room, subject to the constraints of gravity. An example is given on Fig. 4. Typically, we ask for the cubes to be contained inside a bigger box (parallelepiped) of given sizes.

Alternatively, one can project the picture onto a two-dimensional plane (which is inevitably what we do when we draw the picture on paper) and the result is a tiling of a region of the plane by lozenges (or rhombi) of three possible orientations, as shown on the right of the figure. If the cubes are inside a parallelepiped of size $a \times b \times c$, then, possibly drawing the walls of the room as extra tiles, we obtain a lozenge tiling of a hexagon with sides a, b, c , which is the situation we consider now.

1.4.2. *MacMahon formula.* In order to display the free fermionic nature of plane partitions, we shall consider the following operation. In the 3D view, consider slices of the piling of boxes by hyperplanes parallel to two of the three axis and such that they are located halfway between successive rows of cubes. In the 2D view, this corresponds to selecting two orientations among the three orientations of the lozenges and building paths out of these. Fig. 5 shows on the left the result of such an operation: a set of lines going from one side to

the opposite side of the hexagon. They are by definition non-intersecting and can only move in two directions. Inversely, any set of such NILPs produces a plane partition.

At this stage one can apply the LGV formula. But there is no need since this is actually the case already considered in section 1.3.4. Compare Figs. 5 and 1: the trajectories of holes are exactly our paths (in fact, it is left to the reader as an exercise to check that the trajectories of particles form another set of NILPs corresponding to another choice of two orientations of lozenges; what about the third choice?). If we attach a weight of x_i to each blue lozenge at step i , we find that the weighted enumeration of plane partitions in a $a \times b \times c$ box is given by:

$$N_{a,b,c}(x_1, \dots, x_{a+b}) = \langle 0 | e^{H[t]} | b \times c \rangle = s_{b \times c}(x_1, \dots, x_{a+b})$$

where $b \times c$ is the rectangular Young diagram with height b and width c . In particular the unweighted enumeration is the dimension of the Young diagram $b \times c$ as a $GL(a+b)$ representation:

$$N_{a,b,c} = \prod_{i=1}^a \prod_{j=1}^b \prod_{k=1}^c \frac{i+j+k-1}{i+j+k-2}$$

which is the celebrated MacMahon formula. But the more general formula provides various refinements. For example, one can assign a weight of q to each cube in the 3D picture. It is left as an exercise to show that this is achieved by setting $x_i = q^{-i}$ (up to a global power of q). This way we find the q -deformed formula

$$N_{a,b,c}(q) = \prod_{i=1}^a \prod_{j=1}^b \prod_{k=1}^c \frac{1 - q^{i+j+k-1}}{1 - q^{i+j+k-2}}$$

Many more formulae can be obtained in this formalism. The reader may for example prove that

$$N_{a,b,c} = \sum_{\lambda: \lambda_1 \leq c} s_{\lambda}(\underbrace{1, \dots, 1}_a) s_{\lambda}(\underbrace{1, \dots, 1}_b)$$

or that

$$N_{a,b,c} = \det(1 + T_{c \times b} T_{b \times a} T_{a \times c})$$

(where $T_{y \times x}$ is the matrix with y rows and x columns and entries $\binom{i}{j}$, $i = 0, \dots, y-1$, $j = 0, \dots, x-1$), as well as investigate their possible refinements. (for more formulae similar to the last one, see [39]).

Note that our description in terms of paths clearly breaks the threefold symmetry of the original hexagon. It strongly suggests that one should be able to introduce *three* series of parameters x_1, \dots, x_{a+b} , y_1, \dots, y_{b+c} , z_1, \dots, z_{a+b} to provide an even more refined counting of plane partitions. With two sets of parameters, this is in fact known in the combinatorial literature and is related to so-called double Schur functions (see for example [20] and references therein), which are essentially a form of supersymmetric Schur functions. The full 3-parameter generalization is less well-known and appears in [49], making use of triple Schur functions (see [29] for a definition of multiple Schur functions).

Plane partitions exhibit interesting phenomena in the continuum limit, including spatial phase separation [22], but these will be discussed in Kenyon's lectures.

Remark: as the name suggests, plane partitions are higher dimensional versions of partitions, that is of Young diagrams. After all, each slice we have used to define our NILPs is

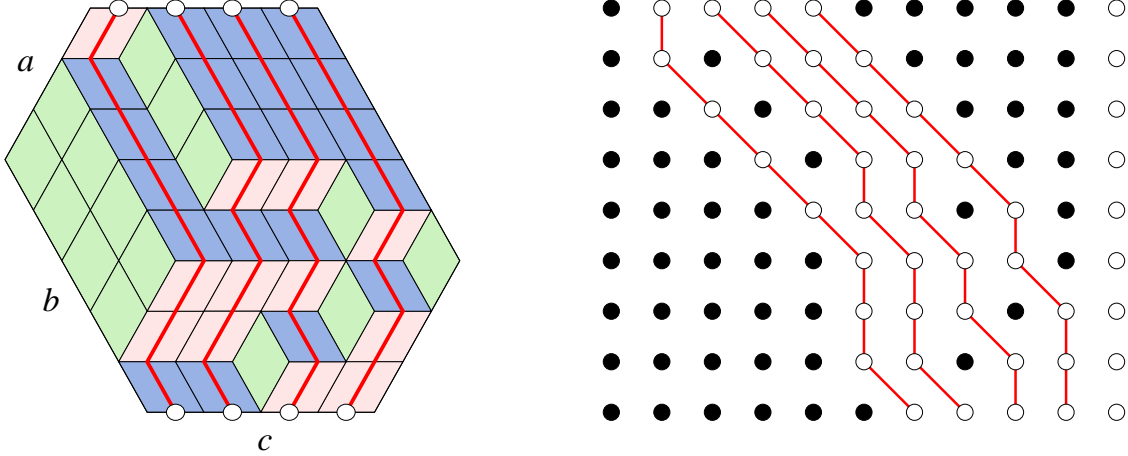


FIGURE 5. NILPs corresponding to a plane partition.

also a Young diagram itself. However these Young diagrams should not be confused with the ones obtained from the NILPs by the correspondence of section 1.3.

1.4.3. *Totally Symmetric Self-Complementary Plane Partitions.* In the mathematical literature, many more complicated enumeration problems are addressed, see [5]. In particular, consider lozenge tilings of a hexagon of shape $2a \times 2a \times 2a$. One notes that there is a group of transformations acting naturally on the set of configurations. We consider here the dihedral group of order 12 which consists of rotations of $\pi/3$ and reflections w.r.t. axis going through opposite corners of the hexagon or through middles of opposite edges. To each of its subgroups one can associate an enumeration problem.

Here we discuss only the case of maximal symmetry, i.e. the enumeration of Plane Partitions with the dihedral symmetry. They are called in this case Totally Symmetric Self-Complementary Plane Partitions (TSSCPPs). The fundamental domain is a twelfth of the hexagon, see Fig. 6. Inside this fundamental domain, one can use the equivalence to NILPs by considering green and blue lozenges. However it is clear that the resulting NILPs are not of the same type as those considered before for general plane partitions, for two reasons: (a) the starting and ending points are not on parallel lines, and (b) the endpoints are in fact free to lie anywhere on a vertical line. However the LGV formula still holds. For future purposes we provide an integral formula for the counting of TSSCPPs [51], where a weight τ is attached to every blue lozenge in the fundamental domain.

Let us call r_j the location of the endpoint of the j^{th} path, numbered from top to bottom starting at zero. We first apply the LGV formula to write the number of NILPs with given endpoints to be $\det(N_{i,r_j})_{1 \leq i,j \leq n-1}$ where $N_{i,r} = \tau^{2i-r-1} \binom{i}{2i-r-1} = (1 + \tau u)^i |_{u^{2i-r-1}}$. Next we sum over them and obtain

$$\begin{aligned}
 (27) \quad N_n(\tau) &= \sum_{0 \leq r_1 < r_2 < \dots < r_{n-1}} \det[(1 + \tau u_i)^i u_i^{r_j}] \Big|_{\prod_{i=1}^{n-1} u_i^{2i-1}} \\
 &= \prod_{i=1}^{n-1} (1 + \tau u_i)^i \sum_{0 \leq r_1 < r_2 < \dots < r_{n-1}} \det(u_i^{r_j}) \Big|_{\prod_{i=1}^{n-1} u_i^{2i-1}}
 \end{aligned}$$

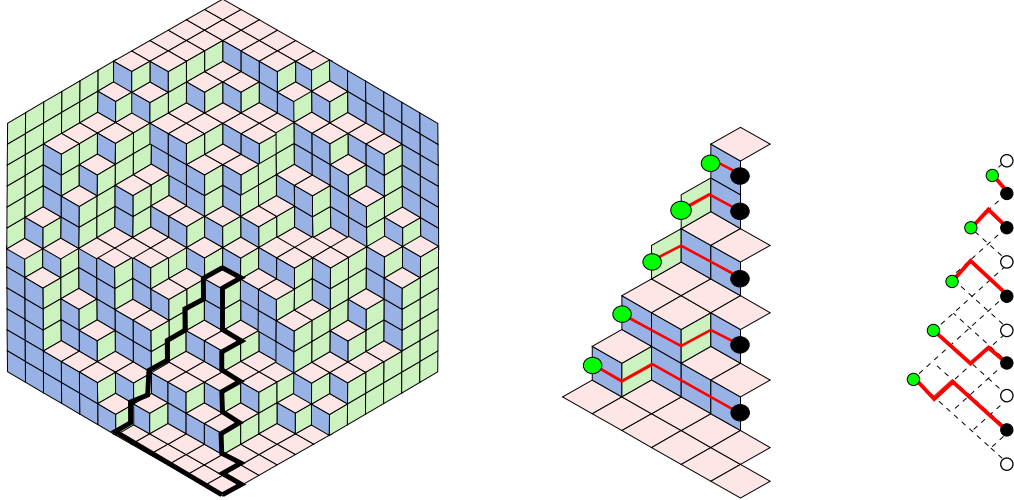


FIGURE 6. A TSSCPP and the associated NILP.

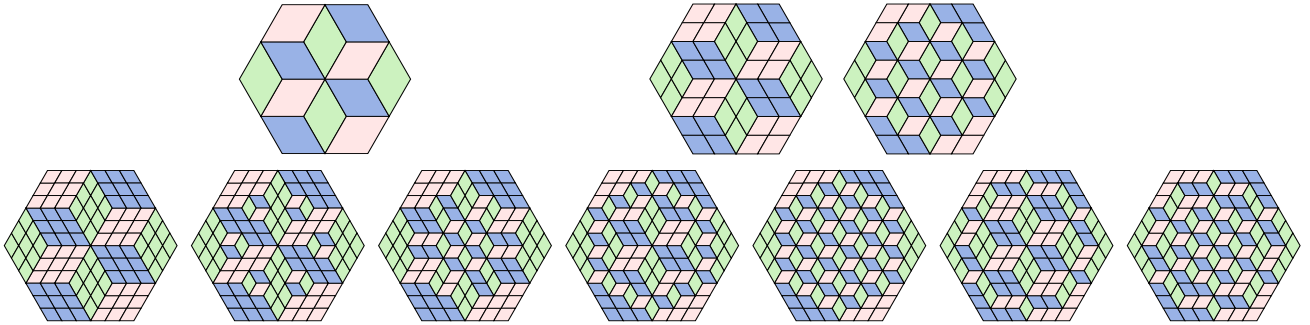


FIGURE 7. All TSSCPPs of size 1, 2, 3.

We recognize the numerator of a Schur function; the summation is simply over all Young diagrams with n parts. At this stage we use a classical summation formula to conclude that

$$(28) \quad N_n(\tau) = \prod_{1 \leq i < j \leq n-1} \frac{u_j - u_i}{1 - u_i u_j} \prod_{i=1}^{n-1} \frac{(1 + \tau u_i)^i}{1 - u_i} \Big|_{\prod_{i=1}^{n-1} u_i^{2i-1}}$$

This formula can be used to generate efficiently these numbers by computer; we find

$$N_n(1) = 1, 2, 7, 42, 429 \dots$$

which have only small prime factors; this allows to conjecture a simple product form:

$$N_n(1) = \prod_{i=0}^{n-1} \frac{(3i+1)!}{(n+i)!} = \frac{1!4! \dots (3n-2)!}{n!(n+1)! \dots (2n-1)!}$$

which was in fact proven in [15]. We shall later provide an actual derivation of this evaluation.

1.4.4. *More general dynamics.* The dynamics we used here are rather trivial (simplest rules for hopping, translational invariance). Many 1D discrete models turn out to be equivalent to free fermions, with possibly more general Hamiltonians. An example that has become popular is the Totally ASymmetric Exclusion Process (TASEP), cf Majumdar's lectures.

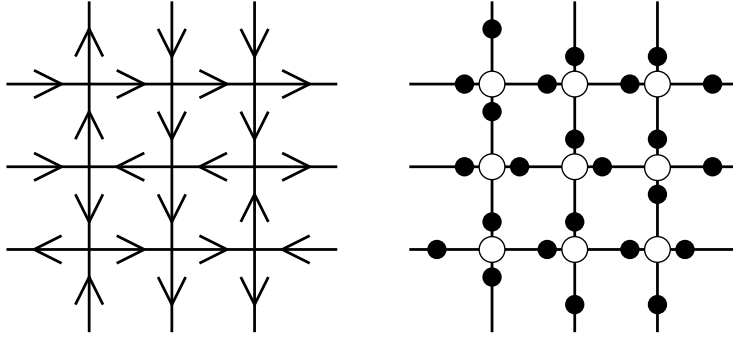


FIGURE 8. A configuration of the six-vertex model.

Another possible variation is to consider particles on a half-line, which corresponds to a neutral fermion, see for example [54, 59].

However, the most interesting models usually involve interactions between fermions and the methods presented here no longer apply. These models however remain often quantum integrable – typically, large classes of fermionic models with four-fermion interaction are integrable. The six-vertex model described in the next section can in fact be formulated in such a way. The general Partial ASymmetric Exclusion Process (PASEP) [13, 14, 16] is also of this type.

1.5. Classical integrability. The free fermionic Fock space is also important for the construction of solutions of *classically integrable* hierarchies. We refer to [6] and references therein for details. Here we only mention in passing the basic idea since lack of time prevented this from being discussed during the lectures. Recall the isomorphism $\Phi \mapsto \langle \ell | e^{H[t]} | \Phi \rangle$ from \mathcal{F}_ℓ to the space of polynomials in the variables t_q (or equivalently to the space of symmetric functions if the t_q are interpreted as power sums). The resulting symmetric function will be a τ -function of the Kadomtsev–Petviashvili (KP) hierarchy (as a function of the t_q) for appropriately chosen $|\Phi\rangle$. By appropriately chosen we mean the following.

In the first quantized picture, the essential property of free fermions is the possibility to write their wave function as a Slater determinant; this amounts to considering states which are exterior products of one-particle states. Geometrically this is interpreted as saying that the state (defined up to multiplication by a scalar) really lives in a subspace of the full Hilbert space called a Grassmannian. The equations defining this space (Plücker relations) are quadratic; these equations are differential equations satisfied by $\langle \ell | e^{H[t]} | \Phi \rangle$. They are Hirota’s form of the equations defining the KP hierarchy.

2. THE SIX-VERTEX MODEL

The six-vertex model will be presented in great detail in N. Reshetikhin’s lectures. Here we provide the minimum information on the model.

2.1. Definition.

2.1.1. Configurations. The six-vertex model is defined on a (subset of the) square lattice by putting arrows (two possible directions) on each edge of the lattice, with the additional rule that at each vertex, there are as many incoming arrows as outgoing ones. See Fig. 8 for an

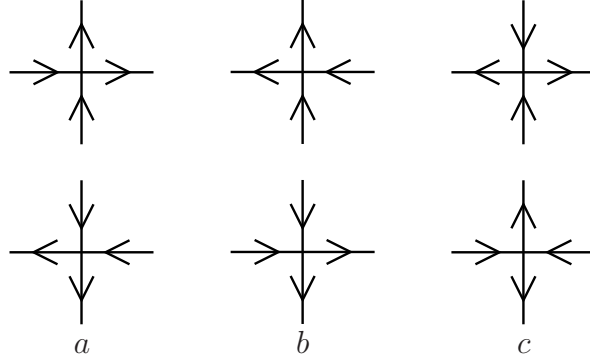


FIGURE 9. Weights of the six-vertex model.

example, and for an alternative description (“square ice”). Around a given vertex, there are only 6 configurations of edges which respect the arrow conservation rule, see Fig. 9, hence the name of the model.

2.1.2. *Weights.* Let us consider Boltzmann weights that are invariant by reversal of every arrow. The weights are assigned to the six vertices and are traditionally called a , b , c , see Fig. 9. Thus the partition function is given by

$$Z = \sum_{\text{configurations}} \prod_{\text{vertex}} (\text{weight of the vertex})$$

An additional remark is useful. With any fixed boundary conditions, one can show that the difference between the numbers of vertices of the two types c is constant (independent of the configuration). This means that one can actually give different weights c_1 and c_2 to them: only the product $c^2 = c_1 c_2$ will matter. This will be used in what follows.

There is another way to formulate the partition function, using a transfer matrix. In order to set up a transfer matrix formalism, we first need to specify the boundary conditions. Let us consider doubly periodic boundary conditions in the two directions of the lattice, so that the model is defined on lattice of size $M \times L$ with the topology of a torus. Then one can write

$$Z = \text{tr } T_L^M$$

where T_L is the $2^L \times 2^L$ transfer matrix which corresponds to a periodic strip of size L . In other words the indices of the matrix T_L are sequences of L up/down arrows. T_L can itself be expressed as a product of matrices which encode the vertex weights; in the case of integrable models, we usually denote this matrix by the letter R :

$$(29) \quad R = \begin{matrix} & \rightarrow\uparrow & \rightarrow\downarrow & \leftarrow\uparrow & \leftarrow\downarrow \\ \begin{matrix} \rightarrow\uparrow \\ \rightarrow\downarrow \\ \leftarrow\uparrow \\ \leftarrow\downarrow \end{matrix} & \begin{pmatrix} a & 0 & 0 & 0 \\ 0 & b & c & 0 \\ 0 & c & b & 0 \\ 0 & 0 & 0 & a \end{pmatrix} \end{matrix}$$

Then we have

$$(30) \quad T_L = \text{tr}_0 R_{0L} \cdots R_{02} R_{01} = \cdots \begin{array}{c|c|c|c|} \hline & & & \\ \hline 0 & 1 & 2 & 3 & 4 \\ \hline & & & & \\ \hline \end{array} \cdots$$

where R_{ij} means the matrix R acting on the tensor product of i^{th} and j^{th} spaces, and 0 is an additional auxiliary space encoding the horizontal edges, as on the picture (note that the trace is on the auxiliary space and graphically means that the horizontal line reconnects with itself). On the picture “time” flows upwards and to the right.

2.2. Integrability.

2.2.1. *Properties of the R-matrix.* Let us now introduce the following parameterization of the weights:

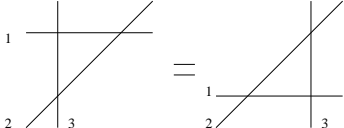
$$(31) \quad \begin{aligned} a &= qx - q^{-1}x^{-1} \\ b &= x - x^{-1} \\ c &= q - q^{-1} \end{aligned}$$

x, q are enough to parameterize them up to global scaling. Instead of q one often uses

$$\Delta = \frac{a^2 + b^2 - c^2}{2ab} = \frac{q + q^{-1}}{2}$$

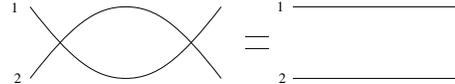
In general, q or Δ are fixed whereas x is a variable parameter, called spectral parameter. It can be thought itself as a ratio of two spectral parameters attached to the lines crossing at the vertex.

The matrix $R(x)$ then satisfies the following remarkable identity: (Yang–Baxter equation)

$$R_{12}(x_2/x_1)R_{13}(x_3/x_1)R_{23}(x_3/x_2) = R_{23}(x_3/x_2)R_{13}(x_3/x_1)R_{12}(x_2/x_1)$$


This is formally the same equation that is satisfied by S matrices in an integrable field theory (field theory with factorized scattering, i.e. such that every S matrix is a product of two-body S matrices).

The R -matrix also satisfies the unitarity equation:

$$R_{12}(x)R_{21}(x^{-1}) = (qx - q^{-1}x^{-1})(qx^{-1} - q^{-1}x)I$$


with $x = x_2/x_1$. The scalar function could of course be absorbed by appropriate normalization of R .

2.2.2. *Commuting transfer matrices.* Consider now the transfer matrix as a function of the spectral parameter x :

$$T_L(x) = \text{tr}_0 R_{0L}(x) \cdots R_{02}(x)R_{01}(x)$$

Then using the Yang–Baxter equation repeatedly one obtains the relation

$$[T_L(x), T_L(x')] = 0$$

We thus have an infinite family of commuting operators. In practice, for a finite chain $T_L(x)$ is a Laurent polynomial of x so there is a finite number of independent operators.

Note that we could have used the more general *inhomogeneous* transfer matrix

$$T_L(x_0; x_1, \dots, x_L) = \text{tr}_0 R_{0L}(y_L/x_0) \cdots R_{02}(y_2/x_0)R_{01}(y_1/x_0)$$

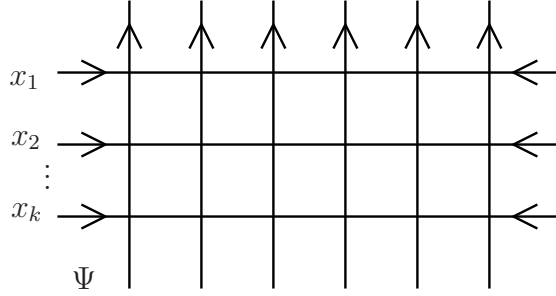


FIGURE 10. A Bethe state.

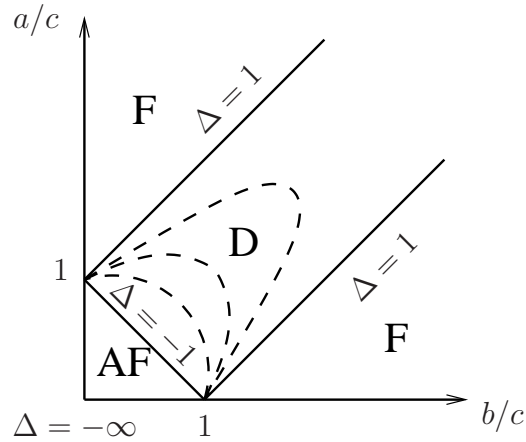


FIGURE 11. Phase diagram of the six-vertex model.

where now we have spectral parameters y_i attached to each vertical line i and one more parameter x_0 attached to the auxiliary line. Then the same commutation relations hold for fixed y_i and variable x_0 .

2.2.3. Bethe Ansatz. We do not discuss here the Bethe Ansatz, since it will be developed in other lectures. Roughly, the (Algebraic) Bethe Ansatz [3, 18] consists in considering states Ψ of the form of Fig. 10, and choosing appropriately the parameters x_1, \dots, x_k in such a way that Ψ is an eigenvector of the transfer matrix. This turns out to be equivalent to imposing some algebraic equations (Bethe equations) on the x_i .

In the case of the largest eigenvalue of the transfer matrix, one can solve exactly the Bethe equations in the limit where the size of the system goes to infinity. This gives access to the bulk free energy, which allows to describe the phase diagram.

2.3. Phase diagram. We find the following phase diagram, based on the exact solution of the model. The physical properties of the system depend only on $\Delta = (q + q^{-1})/2$, x playing the role of a lattice anisotropy parameter. We distinguish three phases, see Fig. 11:

2.3.1. $\Delta \geq 1$: Ferroelectric phase. This phase is non-critical. Furthermore, there are no local degrees of freedom: the system is frozen in regions filled with one of the vertices of type a or b (i.e. all arrows aligned), and no local changes (that respect arrow conservation) are possible.

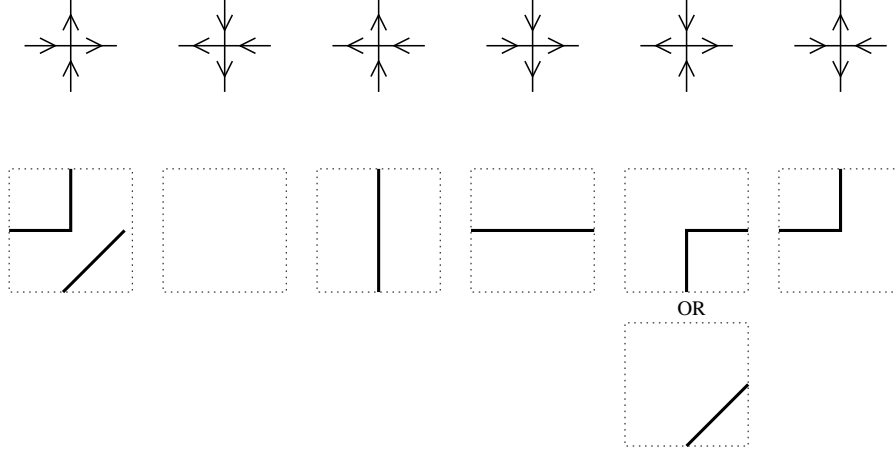


FIGURE 12. From $\Delta = 0$ six-vertex to NILPs.

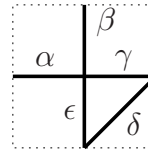
2.3.2. $\Delta < -1$: *Antiferroelectric phase*. This phase is non-critical. This time there is a finite correlation length. The ground state of the transfer matrix corresponds to a state with zero polarization (in the limit $\Delta \rightarrow -\infty$, it is simply an alternation of up and down arrows).

2.3.3. $-1 \leq \Delta < 1$: *Disordered phase*. This phase is critical. It possesses a continuum limit with conformal symmetry, and this limiting infra-red Conformal Field Theory is well-known: it is simply the $c = 1$ theory of a free boson on a circle with radius R given by

$$R^2 = \frac{1}{2(1 - \gamma/\pi)} \quad \Delta = -\cos \gamma$$

In other words, it is a bosonic field $\varphi(z, \bar{z})$ with $\varphi \equiv \varphi + 2\pi R$ and action $\frac{1}{2\pi} \int d^2z \partial\varphi \bar{\partial}\varphi$. The primary operators for the underlying chiral algebras are the electro-magnetic vertex operators $e^{i(\frac{n}{R}\varphi + mR\bar{\varphi})}$ with conformal weight $\Delta = \frac{1}{8}m^2R^2 + \frac{1}{2}\frac{n^2}{R^2}$. These are discussed in detail in Nienhuis' lectures, and we shall not go further in this direction.

2.3.4. *Free fermion point*. Inside the disordered phase, there is a special point $\Delta = 0$. By combining the equivalences of [41] and [27], one can provide a NILP representation of the six-vertex model at $\Delta = 0$, thus showing it is a system of free fermions. This is described on Fig. 12. Note that the correspondence is not one-to-one: one of the c vertices corresponds to two possible local paths.



The directed graph of the NILPs is the basic pattern repeated, with paths moving upwards and to the right, and with weights indicated on the edges. Comparing the weights we get the relations

$$\begin{aligned} a &= \alpha\beta\delta = 1 \\ b &= \alpha\gamma = \beta\epsilon \\ c_1 &= \epsilon\gamma + \delta \\ c_2 &= \alpha\beta \end{aligned}$$

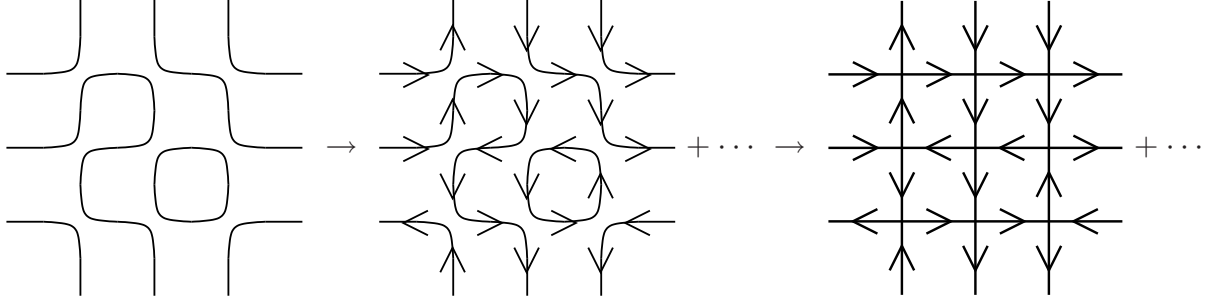


FIGURE 13. From CPLs to six-vertex.

Combining these we find that $a^2 + b^2 - c_1 c_2 = 0$, so the correspondence only makes sense at $\Delta = 0$.

2.4. Equivalence to loop models. Here we follow the terminology of B. Nienhuis' lectures concerning loop models.

2.4.1. Completely Packed Loops. In order to go from the six-vertex model to Completely Packed Loops (CPL), one can first transform the six-vertex model into a height model and then apply the general spin model–loop model correspondence à la Pasquier [10]. Since this approach was emphasized by B. Nienhuis, we shall use here another (strictly equivalent) route. An example is shown on Fig. 13.

Start from a CPL configuration. One can introduce a local weight of u for one of the two types of CPL vertices, say NE/SW loops. Furthermore, the (unoriented) loops carry a weight of n . A convenient way to make the latter weight also local is to turn unoriented loops into *oriented loops*: each configuration is now expanded into $2^{\# \text{ loops}}$ configurations with every possible orientation of the loops. The weight of a 90 degrees turn is chosen to be $\omega^{\pm 1/4}$, where $n = \omega + \omega^{-1}$.

Finally we forget about the original loops, retaining only the arrows. We note that the arrow conservation is automatically satisfied around each vertex: we thus obtain one of the six vertex configurations.

$$\begin{aligned}
 a &= \begin{array}{c} \nearrow \\ \rightarrow \\ \searrow \end{array} = \begin{array}{c} \leftarrow \\ \uparrow \\ \searrow \end{array} = u \\
 b &= \begin{array}{c} \nearrow \\ \leftarrow \\ \searrow \end{array} = \begin{array}{c} \rightarrow \\ \uparrow \\ \downarrow \end{array} = 1 \\
 c_1 &= \begin{array}{c} \nearrow \\ \leftarrow \\ \rightarrow \end{array} + \begin{array}{c} \leftarrow \\ \rightarrow \\ \searrow \end{array} = u\omega^{1/2} + \omega^{-1/2} \quad c_2 = \begin{array}{c} \nearrow \\ \downarrow \\ \searrow \end{array} + \begin{array}{c} \rightarrow \\ \uparrow \\ \downarrow \end{array} = \omega^{1/2} + u\omega^{-1/2}
 \end{aligned}$$

Note that if $u = 1$ all weights become rotationally invariant and $a = b$, $c_1 = c_2$.

Finally, one checks that the formula $\Delta = -n/2$ holds (equivalently $q = -\omega$), u playing the role of spectral parameter. In particular the critical phase $|\Delta| < 1$ corresponds to $|n| < 2$.

Remark: this construction only works in the plane. On the cylinder or on the torus we have a problem: there are non-contractible loops which according to the prescription above get a weight of 2. We shall not discuss here how to correct this (see section 3.1.3); we simply note that this explains the discrepancy of central charges between 6-vertex model ($c = 1$) and CPL ($c < 1$).

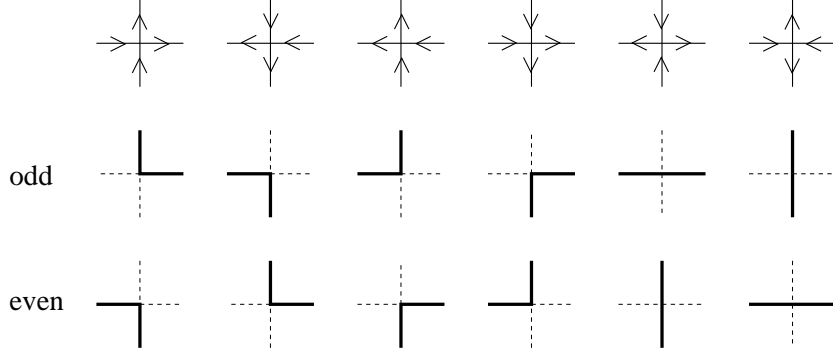


FIGURE 14. From six-vertex to FPLs.

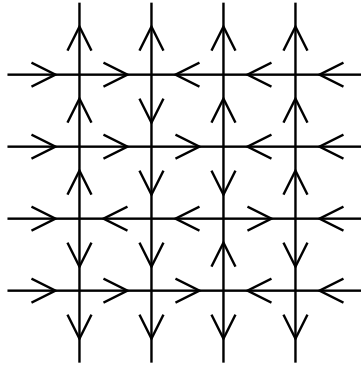


FIGURE 15. An example of configuration with Domain Wall Boundary Conditions.

2.4.2. *Fully Packed Loops.* There is a more limited relation to the model of Fully Packed Loops (FPL). The limitation comes from the fact that one cannot assign an actual weight to the loops, so that we only obtain an $n = 1$ model. This time the correspondence between configurations is one-to-one: starting from the six-vertex model side, one imposes that at every vertex, arrows pointing in the same direction should be in the same state (occupied or empty) on the FPL side. This forces us to distinguish odd and even sublattices, and leads to the rules of Fig. 14.

For rotational invariance of the FPL weights one should have $a = b$. c/a then has a meaning of “rigidity” parameter of the loops.

2.5. Domain Wall Boundary Conditions. Domain Wall Boundary Conditions (DWBC) were special boundary conditions which were originally introduced in order to study correlation functions of the six-vertex model [4]. However they are also interesting in their own right.

2.5.1. *Definition.* DWBC are defined on a $n \times n$ square grid: all the external edges of the grid are fixed according to the rule that vertical ones are outgoing and horizontal ones are incoming. An example is given on Fig. 15.

To each horizontal (resp. vertical) line one associates a spectral parameter x_i (resp. y_j). The partition function is thus:

$$Z_n(x_1, \dots, x_n; y_1, \dots, y_n) = \sum_{\text{configurations}} \prod_{i,j=1}^n w(y_j/x_i)$$

where $w = a, b, c$ depending on the type of vertex.

2.5.2. *Korepin's recurrence relations.* In [4], a way to compute Z_n inductively was proposed. It is based on the following properties:

- $Z_1 = q - q^{-1}$.
- $Z_n(x_1, \dots, x_n; y_1, \dots, y_n)$ is a symmetric function of the $\{x_i\}$ and of the $\{y_i\}$ (separately). This is a consequence of the Yang-Baxter equation:

$$(q y_{i+1}/y_i - q^{-1} y_i/y_{i+1}) Z_n(\dots, y_i, y_{i+1}, \dots) = (q y_{i+1}/y_i - q^{-1} y_i/y_{i+1}) Z_n(\dots, y_{i+1}, y_i, \dots)$$

and similarly for the x_i .

- Z_n multiplied by x_i^{n-1} (resp. y_i^{n-1}) is a polynomial of degree at most $n - 1$ in each variable x_i^2 (resp. y_i^2). This is because (i) each variable say x_i appears only on row i (ii) a, b are linear combinations of x_i^{-1}, x_i and c is a constant and (iii) there is at least one vertex of type c on each row/column.
- The Z_n obey the following recursion relation:

$$(32) \quad Z_n(x_1, \dots, x_n; y_1 = x_1, \dots, y_n) = (q - q^{-1}) \prod_{i=2}^n (q x_1/x_i - q^{-1} x_i/x_1) \prod_{j=2}^n (q y_j/x_1 - q^{-1} x_1/y_j) Z_{n-1}(x_2, \dots, x_n; y_2, \dots, y_n)$$

Since $y_1 = x_1$ implies $b(y_1/x_1) = 0$, by inspection all configurations with non-zero weights are of the form shown on Fig. 16. This results in the identity.

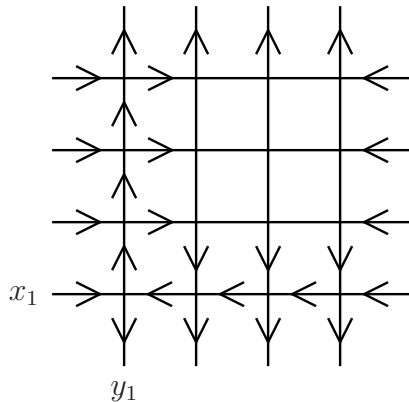


FIGURE 16. Graphical proof of the recursion relation.

Note that by the symmetry property, Eq. (32) fixes Z_n at n distinct values of y_1 : x_i , $i = 1, \dots, n$. Since Z_n is of degree $n - 1$ in y_1^2 , it is entirely determined by it.

2.5.3. *Izergin's formula.* Remarkably, there is a closed expression for Z_n due to Izergin [9, 12]. It is a determinant formula:

$$(33) \quad Z_n = \frac{\prod_{i,j=1}^n (x_j/y_i - y_i/x_j)(q x_j/y_i - q^{-1} y_i/x_j)}{\prod_{1 \leq i < j \leq n} (x_i/x_j - x_j/x_i)(y_i/y_j - y_j/y_i)} \det \left(\frac{q - q^{-1}}{(x_j/y_i - y_i/x_j)(q x_j/y_i - q^{-1} y_i/x_j)} \right)_{i,j=1 \dots n}$$

The hard part is finding the formula, but once it is found, it is a simple check to prove that it satisfies all the properties of the previous section and in particular the recurrence relations (left as an exercise).

2.5.4. *Relation to classical integrability and random matrices.* The Izergin determinant formula is curious because it involves a simple determinant, which reminds us of free fermionic models. And indeed it turns out that it can be written in terms of free fermions, or equivalently that it provides a solution to a hierarchy of classically integrable PDE, in the present case the two-dimensional Toda lattice hierarchy. Due to lack of time this was not discussed during the lectures and we refer to [27].

2.5.5. *Thermodynamic limit.* The six-vertex model suffers from a strong dependence on boundary conditions due to the constraints imposed by arrow conservation. In particular there is no thermodynamic limit in the usual sense (i.e. independently of boundary conditions). This was observed in [26, 27] where the bulk free energy with DWBC was computed and found to be different from that with periodic boundary conditions. In [35] it was suggested that the six-vertex model undergoes spatial phase separation, similarly to dimer models that will be discussed in R. Kenyon's lectures. This was motivated by some numerical evidence, as well as by the exact result at the free fermion point $\Delta = 0$, at which the arctic circle theorem [23] applies: the boundary between phases is known exactly to be an ellipse (a circle for $a = b$) tangent to the four sides of the square.

Since then, there has been a considerable amount of work in this area. There has been more numerical work [42]. The results of [26] have been proven rigorously and extended using sophisticated machinery in the series of papers [47, 57, 60] by Bleher et al. Finally, the curve separating phases has been studied in a series of papers by Colomo and Pronko

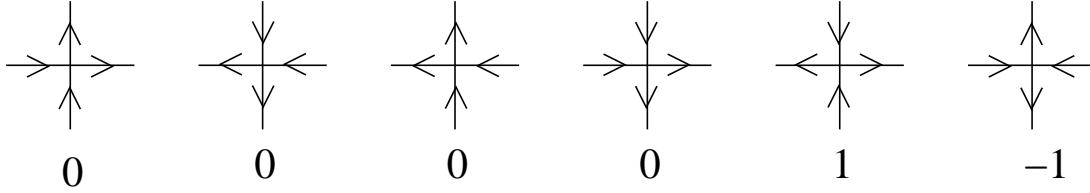


FIGURE 17. From six-vertex to ASMs.

[52, 55], and recently they proposed equations for this curve in the cases $a = b$, $\Delta = \pm 1/2$ [62].

2.5.6. *Application: Alternating Sign Matrices.* *Alternating Sign Matrices* are another important object in enumerative combinatorics. They are defined as follows. An Alternating Sign Matrix (ASM) is a square matrix made of 0s, 1s and -1s such that if one ignores 0s, 1s and -1s alternate on each row and column starting and ending with 1s. For example,

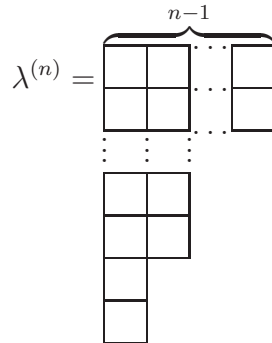
$$\begin{pmatrix} 0 & 1 & 0 & 0 \\ 0 & 0 & 1 & 0 \\ 1 & 0 & -1 & 1 \\ 0 & 0 & 1 & 0 \end{pmatrix}$$

is an ASM of size 4. The enumeration of ASMs is a famous problem with a long history, see [24]. Here we simply note that ASMs are in fact in bijection with six-vertex model configurations with DWBC [21]. The correspondence is quite simple and is summarized on Fig. 17. For example, Fig. 15 becomes the 4×4 ASM above.

We can therefore reinterpret the partition function of the six-vertex model with DWBC as a weighted enumeration of ASMs. It is natural to set the weight of all zeroes to be equal ($a = b$), which leaves us with only one parameter c/a , the weight of a ± 1 . In fact here we shall consider only the pure enumeration problem that is all weights equal. We thus compute $\Delta = 1/2$ and $q = e^{i\pi/3}$, and then $x_i = q$, $y_j = 1$ so that the three weights are $w(x_i/y_j) = q - q^{-1}$.

At this stage there are several options. Either one tries to evaluate directly the formula (33); since the determinant vanishes in the homogeneous limit where all the x_i or y_j coincide, this is a somewhat involved computation and is the content of Kuperberg's paper [21].

There is however a much easier way, discovered independently by Stroganov [34] and Okada [38]. It consists in identifying Z_n at $q = e^{i\pi/3}$ with a Schur function. Consider the partition $\lambda^{(n)} = (n - 1, n - 1, n - 2, n - 2, \dots, 1, 1)$, that is the Young diagram



$s_{\lambda^{(n)}}(z_1, \dots, z_{2n})$ is a polynomial of degree at most $n - 1$ in each z_i (use (25)) and, satisfies the following

$$s_{\lambda^{(n)}}(z_1, \dots, z_j = q^{-2}z_i, \dots, z_n) = \prod_{\substack{k=1 \\ k \neq i, j}}^{2n} (z_k - q^2 z_i) s_{\lambda^{(n-1)}}(z_1, \dots, \hat{z}_i, \dots, \hat{z}_j, \dots, z_{2n})$$

where the hat means that these variables are skipped (start from (14), find all the zeroes as $z_j = q^2 z_i$ and then set $z_i = z_j = 0$ to find what is left).

This looks similar to recursion relations (32). After appropriate identification one finds:

$$Z_n(x_1, \dots, x_n; y_1, \dots, y_n) \Big|_{q=e^{i\pi/3}} = (-1)^{n(n-1)/2} (q - q^{-1})^n \prod_{i=1}^n (q x_i y_i)^{-(n-1)} s_{\lambda^{(n)}}(q^2 x_1^2, \dots, q^2 x_n^2, y_1^2, \dots, y_n^2)$$

Note that Z_n possesses at the point $q = e^{i\pi/3}$ an enhanced symmetry in the whole set of variables $\{q x_1, \dots, q x_n, y_1, \dots, y_n\}$. Finally, setting $x_i = q^{-1}$ and $y_j = 1$ and remembering that this will give a weight of $(q - q^{-1})^{n^2}$ to each ASM, one concludes that the number of ASMs is given by

$$A_n = 3^{-n(n-1)/2} s_{\lambda^{(n)}}(\underbrace{1, \dots, 1}_{2n}) = 3^{-n(n-1)/2} \prod_{1 \leq i < j \leq 2n} \frac{\lambda_i^{(n)} - i - \lambda_j^{(n)} + j}{j - i}$$

Simplifying the product results in

$$(34) \quad A_n = \prod_{i=0}^{n-1} \frac{(3i+1)!}{(n+i)!} = 1, 2, 7, 42, 429 \dots$$

which is a sequence of numbers we have encountered before! In fact, the first proof of formula (34), due to Zeilberger [17], amounts to showing (non-bijectively) that the number of ASMs is the same as the number of TSSCPPs.

These are the ASMs of size 1, 2, 3:

$$\begin{array}{ccccccc} 1 & & & & & & \\ \begin{array}{c} 1 \ 0 \\ 0 \ 1 \end{array} & \begin{array}{c} 0 \ 1 \\ 1 \ 0 \end{array} & & & & & \\ \begin{array}{c} 1 \ 0 \ 0 \\ 0 \ 1 \ 0 \\ 0 \ 0 \ 1 \end{array} & \begin{array}{c} 1 \ 0 \ 0 \\ 0 \ 0 \ 1 \\ 0 \ 1 \ 0 \end{array} & \begin{array}{c} 0 \ 1 \ 0 \\ 1 \ 0 \ 0 \\ 0 \ 0 \ 1 \end{array} & \begin{array}{c} 0 \ 1 \ 0 \\ 0 \ 0 \ 1 \\ 1 \ 0 \ 0 \end{array} & \begin{array}{c} 0 \ 1 \ 0 \\ 1 \ -1 \ 1 \\ 0 \ 1 \ 0 \end{array} & \begin{array}{c} 0 \ 0 \ 1 \\ 1 \ 0 \ 0 \\ 0 \ 1 \ 0 \end{array} & \begin{array}{c} 0 \ 0 \ 1 \\ 0 \ 1 \ 0 \\ 1 \ 0 \ 0 \end{array} \end{array}$$

3. RAZUMOV–STROGANOV CONJECTURE

3.1. Some boundary observables for loop models. Here we go back to a model which was already mentioned (CPL), but with some specific boundary conditions which will play an important role since the observables we shall compute live at the boundary. Several geometries are possible and lead to interesting combinatorial results [36], but here we only consider the case of a cylinder.

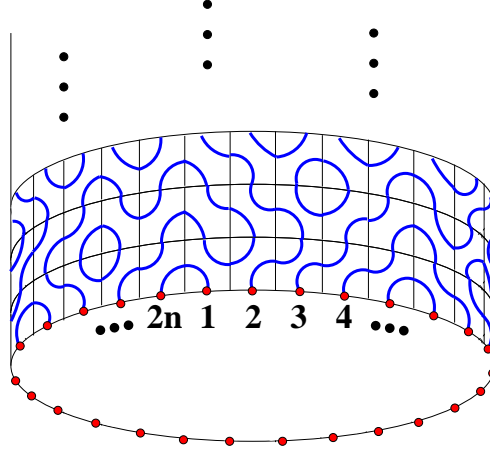


FIGURE 18. The CPL model on a cylinder.

3.1.1. *Loop model on the cylinder.* We consider the model of Completely Packed Loops (CPL) on a semi-infinite cylinder with a finite even number of sites $L = 2n$ around the cylinder, see Fig. 18. It is convenient to draw the dual square lattice of that of the vertices, so that the cylinder is divided into *plaquettes*. Each plaquette can contain one of the two drawings .

We furthermore set $n = 1$, that is we do not put any weights on the loops. There are no more non-local weights, and in fact each plaquette is independent from other plaquettes. So we can reformulate this model as a purely probabilistic model, in which one draws independently at random each plaquette, with say probability p for  and $1 - p$ for .

Finally, we define the observables we are interested in. We consider the *connectivity* of the boundary points, i.e. the endpoints of loops (which are in this case not loops but paths) lying on the the bottom circle. We encode them into connectivity patterns that are called in the literature *link patterns*. In the present context, they can be visualized as follows. Project the cylinder onto a disk in such a way that the boundaries coincide and the infinity is somewhere inside the disk. Remove all loops except the boundary paths. Up to deformation of these resulting paths, what one obtains is a non-crossing pairing of $2n$ points on the boundary of the disk. This is what we call a link pattern of size $2n$; denote their set by P_n . (exercise: show that the number of such link patterns is $c_n = \frac{(2n)!}{n!(n+1)!}$, the so-called Catalan number.) So what we are computing in this model is simply the probability of occurrence of each link pattern. They can be encoded as one vector with c_n entries

$$|\Psi_L\rangle = \sum_{\pi \in P_n} \Psi_\pi |\pi\rangle$$

where P_n is the set of link patterns of size $2n$ and Ψ_π is the probability of link pattern π .

3.1.2. *Markov process on link patterns.* We now show that $|\Psi_L\rangle$ can be reinterpreted as the steady state of a Markov process on link patterns. This is easily understood by considering a transfer matrix formulation of the model. As before let us introduce the transfer matrix that creates one extra row to the semi-infinite cylinder, the important point being that the transfer matrix encodes not the actual plaquettes but the effect of the new plaquettes on the connectivity of the endpoints: that is, we define $T_{\pi, \pi'}(p)$ to be the probability that starting

from a configuration of the cylinder whose endpoints are connected via the link pattern π' and adding a row of plaquettes, one obtains a new configuration whose endpoints are connected via the link pattern π . This form a $c_n \times c_n$ matrix $T_L(p)$.

This transfer matrix is actually stochastic in the sense that

$$(35) \quad \sum_{\pi \in P_n} T_{\pi, \pi'}(p) = 1 \quad \forall \pi'$$

which expresses the conservation of probability. This is of course a special feature of the transfer matrix at $n = 1$. Note that (35) says that $T_L(p)^T$ has eigenvector $(1, \dots, 1)$ with eigenvalue 1.

The matrix $T_L(p)$ has non-negative entries; it is easy to show that it is primitive (the entries of $T_L(p)^n$ are positive). These are the hypotheses of the Perron–Frobenius theorem. Therefore, $T_L(p)$ possesses a unique eigenvector $|\Psi_L\rangle$ with positive entries; the corresponding eigenvalue is positive and is larger in modulus than all other eigenvalues. Now the theorem also applies to $T_L(p)^T$ and by uniqueness we conclude that the largest eigenvalue of $T_L(p)$ and of $T_L(p)^T$ is 1. In conclusion, we find that the eigenvector with positive entries of $T_L(p)$, which with a bit of foresight we call $|\Psi_L\rangle$ again, satisfies

$$(36) \quad T_L(p) |\Psi_L\rangle = |\Psi_L\rangle$$

(In fact the whole reasoning in the previous paragraph is completely general and applies to any Markov process, $|\Psi_L\rangle$ being up to normalization the steady state of the Markov process defined by $T_L(p)$.)

Two more observations are needed. Firstly, (36) is clearly satisfied by the vector of probabilities that we defined in the previous paragraph (the semi-infinite cylinder being invariant by addition of one extra row); it is in fact defined uniquely up to normalization by (36). This explains that we have used the same notation.

Secondly, $|\Psi_L\rangle$ is in fact independent of p . In the next section we obtain this result by going back to the six-vertex model and showing that p plays the role of spectral parameter, so that $[T_L(p), T_L(p')] = 0$. Another proof will be presented when discussing the quantum Knizhnik–Zamolodchikov equation.

3.1.3. Equivalence to the six-vertex model revisited: the space of states. We now show that the transfer matrix we have just defined is essentially the same as the one in section 2.2.2 for the six-vertex model, up to a change of basis and issues of boundary conditions.

We start from the equivalence described in section 2.4.1. The basic idea is to orient the loops. So we start from a link pattern and add arrows to each “loop” (pairing of points). Forgetting about the original link pattern we obtain a collection of $2n$ up or down arrows, which form a state of the 6-vertex model in the transfer matrix formalism. To assign weights it is convenient to think of the points as being on a straight line with the loops emerging perpendicularly: this way each loop can only acquire a weight of $\omega^{\pm 1/2}$, depending on whether

it is moving to the right of to the left. For example, in size $L = 2n = 4$,

$$\begin{aligned}
\begin{array}{c} \text{---} \overset{\text{---}}{\text{---}} \text{---} \\ \text{1} \quad \text{2} \quad \text{3} \quad \text{4} \end{array} &= \omega \begin{array}{c} \text{---} \overset{\text{---}}{\text{---}} \text{---} \\ \text{1} \quad \text{2} \quad \text{3} \quad \text{4} \end{array} + \begin{array}{c} \text{---} \overset{\text{---}}{\text{---}} \text{---} \\ \text{1} \quad \text{2} \quad \text{3} \quad \text{4} \end{array} + \begin{array}{c} \text{---} \overset{\text{---}}{\text{---}} \text{---} \\ \text{1} \quad \text{2} \quad \text{3} \quad \text{4} \end{array} + \omega^{-1} \begin{array}{c} \text{---} \overset{\text{---}}{\text{---}} \text{---} \\ \text{1} \quad \text{2} \quad \text{3} \quad \text{4} \end{array} \\
&= \omega \uparrow_1 \uparrow_2 \downarrow_3 \downarrow_4 + \uparrow_1 \downarrow_2 \uparrow_3 \downarrow_4 + \downarrow_1 \uparrow_2 \downarrow_3 \uparrow_4 + \omega^{-1} \downarrow_1 \downarrow_2 \uparrow_3 \uparrow_4 \\
\begin{array}{c} \text{---} \text{---} \text{---} \text{---} \\ \text{1} \quad \text{2} \quad \text{3} \quad \text{4} \end{array} &= \omega \begin{array}{c} \text{---} \text{---} \text{---} \text{---} \\ \text{1} \quad \text{2} \quad \text{3} \quad \text{4} \end{array} + \begin{array}{c} \text{---} \text{---} \text{---} \text{---} \\ \text{1} \quad \text{2} \quad \text{3} \quad \text{4} \end{array} + \begin{array}{c} \text{---} \text{---} \text{---} \text{---} \\ \text{1} \quad \text{2} \quad \text{3} \quad \text{4} \end{array} + \omega^{-1} \begin{array}{c} \text{---} \text{---} \text{---} \text{---} \\ \text{1} \quad \text{2} \quad \text{3} \quad \text{4} \end{array} \\
&= \omega \uparrow_1 \downarrow_2 \uparrow_3 \downarrow_4 + \uparrow_1 \downarrow_2 \downarrow_3 \uparrow_4 + \downarrow_1 \uparrow_2 \uparrow_3 \downarrow_4 + \omega^{-1} \downarrow_1 \uparrow_2 \downarrow_3 \uparrow_4
\end{aligned}$$

There is only one problem with this correspondence: it is not obviously compatible with periodic boundary conditions. We would like to identify a loop from i to j , $i < j$ and a loop from j to $i + L$, $j < i + L$. This is only possible if we impose *twisted boundary conditions* on the six-vertex model i.e. we assume that $\uparrow_{i+L} = \omega \uparrow_i$, $\downarrow_{i+L} = \omega^{-1} \downarrow_i$. As was explained in Reshetikhin's lectures, this preserves the integrability of the model.

This mapping from the space of link patterns (of dimension c_n) to that of sequences of arrows (of dimension 2^{2n}) is injective; so the space of link patterns is isomorphic to a certain subspace $\mathbb{C}^{2^{2n}}$. The claim, which we shall not prove in detail here but which is a natural consequence of the general formalism is that the transfer matrix of the six-vertex model (defined in section 2.2.2) with the additional twist above leaves invariant this subspace and is identical to the transfer matrix T_L of our loop model up to this isomorphism, the correspondence of weights being the same as in section 2.4.1 (in particular, $\Delta = -n/2$).

All that we have said so far in this paragraph is valid for any values of the parameters. In fine we are only interested in the situation $n = 1$, which is the same as $\Delta = -1/2$ or $q = e^{2\pi i/3}$. Note that this is *not* the same value of Δ ($+1/2$) that was discussed in 2.5.6 in relation with ASMs. p now plays the role of spectral parameter (explicitly, $p = \frac{qx - q^{-1}x^{-1}}{qx^{-1} - q^{-1}x}$). In particular we conclude that $[T_L(p), T_L(p')] = 0$, as announced.

3.2. Properties of the steady state.

3.2.1. *Some empirical observations.* We begin with an example in size $L = 2n = 8$. By brute force diagonalization of the stochastic matrix T_L one obtains the vector $|\Psi_L\rangle$ of probabilities:

$$\begin{aligned}
 |\Psi_8\rangle = & \frac{1}{42} \left(\begin{array}{c} \text{Diagram 1} \\ \text{Diagram 2} \\ \text{Diagram 3} \\ \text{Diagram 4} \end{array} \right) \\
 & + \frac{3}{42} \left(\begin{array}{c} \text{Diagram 5} \\ \text{Diagram 6} \\ \text{Diagram 7} \\ \text{Diagram 8} \end{array} \right) \\
 & + \frac{7}{42} \left(\begin{array}{c} \text{Diagram 9} \\ \text{Diagram 10} \end{array} \right)
 \end{aligned}$$

We recognize some of our favorite numbers A_n , namely 7 and 42.

In fact, Batchelor, de Gier and Nienhuis [30] conjectured the following properties for all system sizes $L = 2n$:

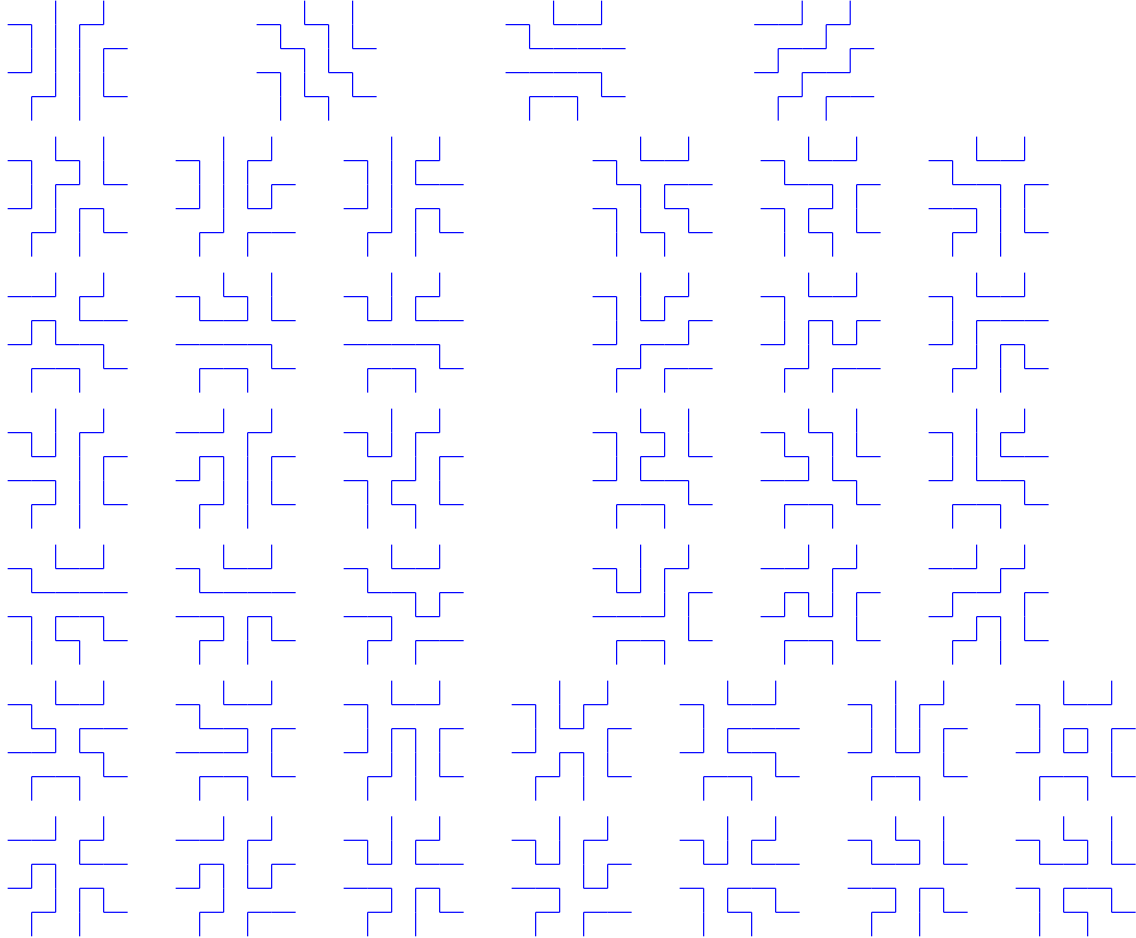
- (1) The smallest probabilities correspond to all pairings being parallel, and equal $1/A_n$.
- (2) All probabilities are integer multiples of the smallest probability.
- (3) The largest probabilities correspond to nearest neighbors being paired and equal A_{n-1}/A_n .

By now all these properties have been proven [40, 51], as will be discussed in section 3.3.

3.2.2. *The general conjecture.* A question however remains: according to property 2 above, if one multiplies the probabilities by A_n , we obtain a collection of integers. The smallest one is 1 and the largest one is A_{n-1} , but what can we say about the other ones?

Recall that A_n also counts the number of six-vertex model configurations with DWBC. Furthermore, we showed that there is a one-to-one correspondence between six-vertex model configurations and FPL configurations (cf section 2.4.2). Let us now draw explicitly the 42

FPLs of size 4×4 :



Note that DWBC translate into the fact that every other external edge is occupied. Interestingly, we find that the reformulation in terms of FPLs allows to introduce once again a notion of connectivity. Indeed, there are $2n$ occupied edges on the exterior square and they are paired by the FPL. We can therefore count separately FPLs with a given link pattern π ; let us denote this by A_π . The Razumov–Stroganov conjecture [32] then states that

$$\Psi_\pi = \frac{A_\pi}{A_n}$$

thus relating two different models of loops (CPL and FPL) with completely different boundary conditions. And even though both models are equivalent to the six-vertex model, the values of Δ are also different (they differ by a sign).

The Razumov–Stroganov conjecture remains open, though some special cases have been proved (e.g. in [49]).

The relation to the conjectured properties of the previous section is as follows. It is easy to show that if π is a link pattern with all pairings parallel, then there exists a unique FPL configuration with connectivity π . Thus the RS conjecture implies property (1). Furthermore, since all A_π are integer, it obviously implies property (2). Property (3) however remains non-trivial, since even assuming the RS conjecture it amounts to saying that $A_\pi = A_{\pi-1}$ in the case of the two link patterns π that pair nearest neighbors, which has not been proven.

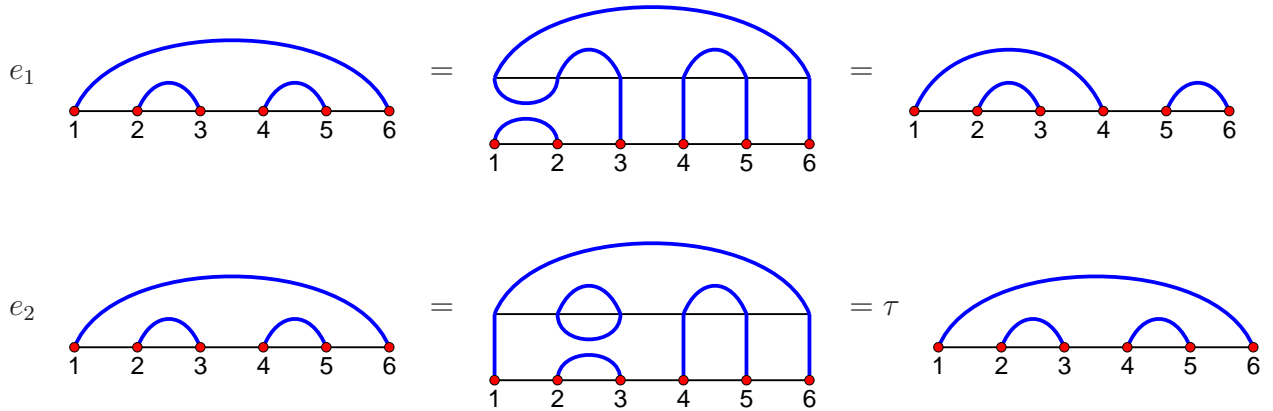
3.3. The quantum Knizhnik–Zamolodchikov equation. We now introduce a new equation whose solution will roughly correspond to a double generalization of the ground state eigenvector $|\Psi_L\rangle$ of the loop model introduced above: (i) it contains inhomogeneities and (ii) it is a continuation of the original eigenvector to an arbitrary value of q , the original value being $q = e^{2\pi i/3}$.

3.3.1. Temperley–Lieb algebra. First we need to define the Temperley–Lieb algebra and its action on the space of link patterns (vector space with canonical basis the $|\pi\rangle$ indexed by link patterns).

The Temperley–Lieb algebra of size L and with parameter τ is given by generators e_i , $i = 1, \dots, L - 1$, and relations:

$$e_i^2 = \tau e_i \quad e_i e_{i\pm 1} e_i = e_i \quad e_i e_j = e_j e_i \quad |i - j| > 1$$

In order to define the action of Temperley–Lieb generators e_i on link patterns, it is simpler to view them graphically as $e_i = \begin{array}{c} \text{---} \\ \cup \\ i \quad i+1 \\ \cap \\ \text{---} \end{array}$; then the relations of the Temperley–Lieb algebra, as well as the representation on the space of link patterns, become natural graphically; for example, we find



where for convenience we flattened link patterns to pairings inside the upper half plane of points on a line. The role of the parameter τ is that each time a closed loop is formed, it can be erased at the price of a multiplication by τ .

In what follows we set $\tau = -(q + q^{-1})$. q is thus a free parameter.

3.3.2. Definition. Introduce once again the R -matrix, but this time rotated 45 degrees and which acts a bit differently than before. Namely, it acts on the vector space spanned by link patterns, in the following way:

$$\check{R}_i(z) = \frac{(q^{-1} - qz)I + (1 - z)e_i}{q^{-1}z - q}$$

Redrawing slightly e_i as $e_i = \begin{array}{c} \diamond \\ \cup \\ \cap \\ \diamond \end{array}$, and similarly $I = \begin{array}{c} \diamond \\ \cup \\ \cup \\ \diamond \end{array}$, we recognize the two (rotated) CPL plaquettes. Note that in this section, it is convenient to use spectral parameters z that are the *squares* of our old spectral parameters x . Indeed, using the equivalence to the

six-vertex model described in section 3.1.3, which amounts to the following representation

$$e_i = \begin{pmatrix} 0 & 0 & 0 & 0 \\ 0 & -q & 1 & 0 \\ 0 & 1 & -q^{-1} & 0 \\ 0 & 0 & 0 & 0 \end{pmatrix}$$

for the Temperley–Lieb generators (acting on the i^{th} and $(i+1)^{\text{st}}$ spaces) we essentially recover the R -matrix of the six-vertex model after the change of variables $z = x^2$:

$$\check{R}(z) = \frac{1}{q x^{-1} - q^{-1} x} \begin{pmatrix} q x - q^{-1} x^{-1} & 0 & 0 & 0 \\ 0 & (q - q^{-1}) x^{-1} & x - x^{-1} & 0 \\ 0 & x - x^{-1} & (q - q^{-1}) x & 0 \\ 0 & 0 & 0 & q x - q^{-1} x^{-1} \end{pmatrix}$$

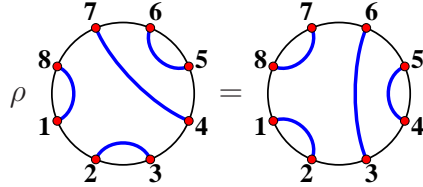
on condition that one perform the following transformations: $\check{R}(z) \propto \mathcal{P} x^{\kappa/2} R(x) x^{-\kappa/2}$ where \mathcal{P} permutes the factors of the tensor product, and $\kappa = \text{diag}(0, 1, -1, 0)$.

Consider now the following system of equations for $|\Psi_L\rangle$, a vector-valued function of the $z_1, \dots, z_L, q, q^{-1}$: ($i = 1, \dots, L-1$)

$$(37) \quad \check{R}_i(z_{i+1}/z_i) |\Psi_L(z_1, \dots, z_L)\rangle = |\Psi_L(z_1, \dots, z_{i+1}, z_i, \dots, z_L)\rangle$$

$$(38) \quad \rho |\Psi_L(z_1, \dots, z_L)\rangle = c |\Psi_L(z_2, \dots, z_L, s z_1)\rangle$$

where ρ rotates link patterns:



and c is a constant that is needed for homogeneity. s is a parameter of the equation: if one sets $s = q^{2(k+\ell)}$ with $k = 2$ (technically, this is the dual Coxeter number of the underlying quantum group), then ℓ is called the *level* of the q KZ equation.

This equation first appeared in [8] in the study of form factors in integrable models. It is not what is usually called the quantum Knizhnik–Zamolodchikov (q KZ) equation; the latter was introduced in [11] as a q -deformation of the Knizhnik–Zamolodchikov (KZ) equation (q KZ is to quantum affine algebras what KZ is to affine algebras). The q KZ equation is of the form

$$(39) \quad S_i(z_1, \dots, z_L) |\Psi_L(z_1, \dots, z_i, \dots, z_L)\rangle = |\Psi_L(z_1, \dots, s z_i, \dots, z_L)\rangle$$

where S_i can be defined pictorially as

$$S_i = \dots \boxed{} \boxed{} \boxed{\text{blue arc}} \boxed{} \boxed{} \dots$$

i

where the empty box is just the “face” graphical representation of the R -matrix (dual to the “vertex” representation we used for the six-vertex model):

$$\boxed{} = \frac{q^{-1} - q z}{q^{-1} z - q} \boxed{\text{blue arc}} + \frac{1 - z}{q^{-1} z - q} \boxed{\text{blue arc}}$$

and the spectral parameters z to be used in S_i are as follows: for the box numbered j , z_j/z_i if $j > i$ or $z_j/(s z_i)$ if $j < i$. Loosely, S_i is the “scattering matrix for the i^{th} particle”.

Alternatively, S_i can be expressed as a product of \check{R}_i and ρ :

$$S_i = \check{R}_{i-1}(z_{i-1}/(s z_i)) \cdots \check{R}_2(z_2/(s z_i)) \check{R}_1(z_1/(s z_i)) \rho \check{R}_{L-1}(z_L/z_i) \cdots \check{R}_{i+1}(z_{i+2}/z_i) \check{R}_i(z_{i+1}/z_i)$$

It is a simple exercise to check using this expression that the system (37–38) implies the q KZ equation (39). Naively, the converse is untrue. However one can show that, up to some transformations, a solution of (39) can always be reduced to a solution of (37–38) (the details are beyond the scope of these lectures).

In what follows we shall only be interested in *polynomial* solutions of the system (37–38).

3.3.3. Relation to affine Hecke algebra. There is an equivalent point of view, which is advocated by Pasquier [43] in the context of the Razumov–Stroganov conjecture.

Start from the q KZ system (37–38), and rewrite it in such a way that the action on the finite-dimensional part (on the space of link patterns) is separated from the action on the variables (on the space of polynomials of L variables). (38) is actually already of this form; (37) needs to be rewritten slightly:

$$(40) \quad (q z_i - q^{-1} z_{i+1}) \partial_i |\Psi_L\rangle = (e_i + q + q^{-1}) |\Psi_L\rangle$$

where $\partial_i \equiv \frac{1}{z_{i+1} - z_i} (\tau_i - 1)$ and τ_i is the operator that switches variables z_i and z_{i+1} , so that the l.h.s. only acts on the polynomial part of $|\Psi_L\rangle$, whereas the r.h.s. only acts on link patterns.

The operators $t_i = (q^{-1} z_{i+1} - q z_i) \partial_i$ acting on polynomials (one should check that t_i acting on a polynomial produces a polynomial) form a representation of the *Hecke algebra* (with parameter $-\tau$); in other words, they satisfy the relations:

$$t_i^2 = -\tau t_i \quad t_i t_{i+1} t_i - t_i = t_{i+1} t_i t_{i+1} - t_{i+1} \quad t_i t_j = t_j t_i \quad |i - j| > 1$$

Equivalently, $t_i + \tau$ satisfies the same relations with $-\tau$ replaced with τ . Note the important fact that the Temperley–Lieb is a quotient of the Hecke algebra. (it is an easy check that the e_i satisfy all the relations of Hecke).

One can add an extra operator on the space of polynomials – the one that appears in the r.h.s. of (38): the cyclic shift r of spectral parameters $z_1 \mapsto z_2 \mapsto \cdots \mapsto z_L \mapsto s z_1$. The t_i together with r generate a representation of the *affine Hecke algebra*.

We can now interpret Eqs. (38–40) as follows: we have on the one hand a representation of the affine Hecke algebra on the space of link patterns (with generators e_i and ρ); and on the other hand a representation of the same algebra on polynomials of L variables (the $t_i + \tau$ and r). $|\Psi_L\rangle$ provides a bridge between these two representations; it is essentially an invariant object in the tensor product of the two, that is it provides a sub-representation of the space of polynomials (explicitly, the span of the Ψ_π) which is isomorphic to the dual of the (irreducible) representation on the link patterns.

So the search for polynomial solutions of (37–38) is equivalent to finding irreducible sub-representations of the action of affine Hecke on the space of polynomials.

Remark: the direct relation between q KZ and representations of an appropriate affine algebra only works for the A_n series of algebras i.e. affine Hecke. For more complicated situations such as the BWM algebra, it fails because one cannot separate the two different actions [46].

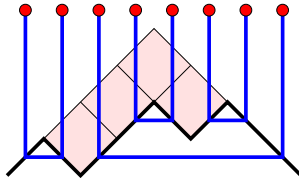


FIGURE 19. From a Young diagram to a link pattern: in this example, from the partition $(2, 1, 1)$ to the pairings $(1, 2), (3, 8), (4, 5), (6, 7)$.

3.3.4. *Polynomial solution.* On general grounds, we only expect polynomial solution for integer values of the level. Here we shall only need a solution at level 1, that is $s = q^6$. Note that the KZ equation at level 1 is essentially connected to free fermions (coming in two species), so that what we shall produce is essentially a q -deformed version of free fermions (the other difference being that we use the basis of link patterns and not the usual basis of the six-vertex model). By comparison with free fermionic formulae, we expect this solution to be of degree $n(n - 1)$.

We shall build this solution in several steps. First, we use a “nice” property of our basis of link patterns, that is, the fact that (40) can be written as a *triangular* linear system in the components of $|\Psi_L\rangle$. This requires to define an order on link patterns, which is most conveniently described as follows. Draw once again link patterns as pairings of points on a line and consider the operation described on Fig. 19. It gives a bijection between link patterns of size $2n$ and Young diagrams inside the staircase diagram $(n - 1, n - 2, \dots, 1)$. Then the order is inclusion of Young diagrams. The smallest element, corresponding to the empty Young diagram, is denoted by π_0 ; it connects i and $L + 1 - i$ (note that it is one of the link patterns with all pairings parallel, which correspond to the smallest probability $1/A_n$ in the loop model). Consider now the exchange equation (40) and write it in components; we find two possibilities:

- i and $i + 1$ are not paired. Then we find that (40) only involves Ψ_π , and implies that $q z_i - q^{-1} z_{i+1}$ divides Ψ_π , and furthermore $\Psi_\pi / (q z_i - q^{-1} z_{i+1})$ is symmetric in the exchange of z_i and z_{i+1} .
- i and $i + 1$ are paired. Then

$$(q z_i - q^{-1} z_{i+1}) \partial_i \Psi_\pi = \sum_{\pi' \neq \pi, e_i \cdot \pi' = \pi} \Psi_{\pi'}$$

that is it involves the sum over preimages of π by e_i viewed as acting on the set of link patterns. It turns out there are two types of preimages of a given π : in terms of Young diagrams, there is the Young diagram obtained from π by adding one box at $i, i + 1$ (which is always possible unless π is the largest element); and there are other Young diagrams that are included in π . So we can write the equation

$$\Psi_{\pi + \text{one box at } (i, i+1)} = (q z_i - q^{-1} z_{i+1}) \partial_i \Psi_\pi - \sum_{\substack{\pi' \subset \pi \\ e_i \cdot \pi' = \pi}} \Psi_{\pi'}$$

which has the desired triangular structure and allows to build the Ψ_π one by one by adding boxes to the corresponding Young diagram. However there is no equation for Ψ_{π_0} . In fact this triangular system can be explicitly solved [25] (see also [56]) in the sense that every Ψ_π can be written as a series of operators acting on Ψ_{π_0} . We shall not need this here.

From the discussion above, we find that all we need is to fix Ψ_{π_0} . We use the following simple observation, which generalizes the first case in the dichotomy above: *if there are no pairings between points $i, i+1, \dots, j$ in π , then $\prod_{i \leq p < q \leq j} (q z_p - q^{-1} z_q)$ divides Ψ_π .* (prove this by induction on $j-i$).

In the case of π_0 , we find $n(n-1)$ factors, which exhausts the expected degree. We therefore make the minimality assumption that Ψ_{π_0} is just

$$(41) \quad \Psi_{\pi_0} = \prod_{1 \leq i < j \leq n} (q z_i - q^{-1} z_j) \prod_{n+1 \leq i < j \leq 2n} (q^{-1} z_j - q z_i)$$

where we recall that the system size is $L = 2n$.

It remains a non-trivial fact that with such a choice of Ψ_{π_0} , (38) is satisfied, with $s = q^6$. We refer to the papers [43, 44] for details.

3.3.5. Connection to the loop model. In general, the two problems of diagonalizing the transfer matrix and finding solutions of q KZ are unrelated. However there is exactly one value of q where a solution of q KZ does in fact provide an eigenvector of the transfer matrix. This is when the parameter $s = 1$ which here occurs when $q = e^{2\pi i/3}$ (other sixth roots of unity are possible but they are either trivial or give the same result as the one we picked). In this case note that (38) becomes a simple rotational invariance condition. Furthermore the real q KZ equation (39) becomes an eigenvector equation for the scattering matrices:

$$S_i(z_1, \dots, z_L) |\Psi_L(z_1, \dots, z_L)\rangle = |\Psi_L(z_1, \dots, z_L)\rangle$$

These scattering matrices do not involve any extra shifts of the spectral parameters, and as is well-known in Bethe Ansatz, are just specializations of the inhomogeneous transfer matrix. Indeed if we define $T_L(z; z_1, \dots, z_L)$ to be simply

$$T_L = z \begin{array}{|c|c|} \hline & \\ \hline z_1 & z_2 \\ \hline \end{array} \cdots \begin{array}{|c|} \hline \\ \hline z_L \\ \hline \end{array}$$

(with periodic boundary conditions) then observe that $S_i(z_1, \dots, z_L) = T(z_i; z_1, \dots, z_L)$. By a Lagrange interpolation argument, we conclude that

$$T_L(z; z_1, \dots, z_L) |\Psi_L(z_1, \dots, z_L)\rangle = |\Psi_L(z_1, \dots, z_L)\rangle$$

i.e. $|\Psi_L\rangle$ is up to normalization the steady state of the inhomogeneous Markov process defined by $T_L(z; z_1, \dots, z_L)$. In order to recover the original homogeneous Markov process, one simply sets all $z_i = 1$.

Note that the normalization is fixed by specifying the value of Ψ_{π_0} ; in particular, if all $z_i = 1$, using (41) we find $\Psi_{\pi_0} = 3^{n(n-1)/2}$, to be compared with the (conjectured) probability $1/A_n$ associated to π_0 . In other words, with this normalization, one should have $\sum_{\pi \in P_n} \Psi_\pi = 3^{n(n-1)/2} A_n$.

3.3.6. Integral formulae. Using the formalism of the q KZ equation allows to prove the properties discussed in 3.2.1, as well as to reconnect the three models that we have found in which the same numbers A_n appear. Recently, a particular useful tool to exploit these solutions of q KZ has been introduced [51, 53, 61]: it consists in writing integral formulae for them.

Here we shall only give the main points and let those who are interested read the papers. We concentrate on one single quantity: the sum of all components of Ψ_π . Then we claim

that the following formula holds:

$$\sum_{\pi \in P_n} \Psi_\pi = (-1)^{n(n-1)/2} \prod_{1 \leq i < j \leq 2n} (q z_i - q^{-1} z_j) \oint \cdots \oint \prod_{\ell=0}^{n-1} \frac{dw_\ell (q w_\ell - z_{2\ell+1})}{2\pi i} \frac{\prod_{0 \leq \ell < m \leq n-1} (w_m - w_\ell) (q w_\ell - q^{-1} w_m)}{\prod_{\ell=0}^{n-1} \prod_{1 \leq i \leq 2\ell+1} (w_\ell - z_i) \prod_{2\ell+1 \leq i \leq 2n} (q w_\ell - q^{-1} z_i)}$$

where the contours surround the z_i counterclockwise, but not the $q^{-2} z_i$.

At this stage one can do two things. On the one hand, one can check directly [61] that $\sum_{\pi \in P_n} \Psi_\pi$, at $q = e^{2\pi i/3}$ equals up to prefactors the partition function of the six-vertex model with DWBC at $q = e^{i\pi/3}$, or equivalently the Schur function $s_{\lambda^{(n)}}$:

$$\sum_{\pi \in P_n} \Psi_\pi(z_1, \dots, z_{2n}) \Big|_{q=e^{2\pi i/3}} = s_{\lambda^{(n)}}(z_1, \dots, z_{2n})$$

We conclude that the steady state probability of the link pattern π_0 is, in the homogeneous case $z_i = 1$, $\Psi_{\pi_0} / (\sum_{\pi \in P_n} \Psi_\pi) = 1/A_n$. More generally we find the probability of link pattern π_0 for arbitrary inhomogeneities.

On the other hand, one can try to set $z_i = 1$ directly in the integral formula; it is convenient to send the two poles (1 and q^{-2}) to zero and infinity respectively by the homographic transformation $u_\ell = (w_\ell - 1)/(q w_\ell - q^{-1})$, and we find:

$$\frac{1}{\Psi_{\pi_0}} \sum_{\pi \in P_n} \Psi_\pi(1, \dots, 1) = \oint \cdots \oint \prod_{\ell=0}^{n-1} \frac{(1 + u_\ell) du_\ell}{2\pi i u_\ell^{2\ell+1}} \prod_{0 \leq \ell < m \leq n-1} (u_m - u_\ell) (1 + \tau u_m + u_\ell u_m)$$

where $\tau = -q - q^{-1}$, and the contours surround zero. This can be rewritten

$$\frac{1}{\Psi_{\pi_0}} \sum_{\pi \in P_n} \Psi_\pi(1, \dots, 1) = \prod_{\ell=0}^{n-1} (1 + u_\ell) \prod_{0 \leq \ell < m \leq n-1} (u_m - u_\ell) (1 + \tau u_m + u_\ell u_m) \Big|_{\prod_{i=1}^{n-1} u_i^{2i}}$$

In fact one can simply set $u_0 = 0$ to get

$$(42) \quad \frac{1}{\Psi_{\pi_0}} \sum_{\pi \in P_n} \Psi_\pi(1, \dots, 1) = \prod_{\ell=1}^{n-1} (1 + u_\ell) \prod_{1 \leq \ell < m \leq n-1} (u_m - u_\ell) (1 + \tau u_m + u_\ell u_m) \Big|_{\prod_{i=1}^{n-1} u_i^{2i-1}}$$

which looks strikingly similar to the formula for the weighted enumeration TSSCPPs (28).

There is however an important difference. Whereas (28) just contains a product of functions of one variable times an antisymmetric function of the u_i (which, ultimately, comes from the free fermionic nature of the model), (42) does not possess any particular symmetry w.r.t. exchange of its variables, due to the factors $1 + \tau u_m + u_\ell u_m$ (which come from the q -deformed Vandermonde product in the original integral formula). One can however antisymmetrize formula (42) [58, 61], and one then recovers (28). The result is a very non-trivial connection which goes beyond the value $q = e^{2\pi i/3}$: for generic q , the sum of components of the solution of q KZ reproduces the weighted enumeration of TSSCPPs with weight $\tau = -q - q^{-1}$, proving a conjecture formulated in [50].

REFERENCES

- [1] P. MacMahon, *Combinatory analysis*, Cambridge University Press (1915).
- [2] B. Lindström, *On the vector representations of induced matroids*, Bull. London Math. Soc. 5 (1973), 85–90.
- [3] L.D. Faddeev, E.K. Sklyanin, L.A. Takhtajan, *Theor. Math. Phys.* 40 (1979), 194.
- [4] V.E. Korepin, *Calculation of norms of Bethe wave functions*, Commun. Math. Phys. 86 (1982), 391.
- [5] R. Stanley, *A baker’s dozen of conjectures concerning plane partitions*, Combinatoire Enumérative (Eds G. Labelle and P. Leroux), Lecture Notes in Math. vol 1234, Springer–Verlag (1986), 285–293.
- [6] M. Jimbo, T. Miwa, *Solitons and Infinite Dimensional Lie Algebras*, Publ. RIMS 19 (1983), 943–1001.
- [7] I.M. Gessel and X. Viennot, *Binomial determinants, paths and hook formulae*, Adv. Math. 58 (1985), 300–321.
- [8] F.A. Smirnov, *A general formula for soliton form factors in the quantum sine-Gordon model*, J. Phys. A 19 (1986), L575–L578.
- [9] A.G. Izergin, *Partition function of a six-vertex model in a finite volume*, Sov. Phys. Dokl. 32 (1987), 878–879.
- [10] V. Pasquier, *Two-dimensional critical systems labelled by Dynkin diagrams*, Nucl. Phys. B 285 (1987), 162.
- [11] I.B. Frenkel and Yu.B. Reshetikhin, *Quantum affine algebras and holonomic difference equations*, Commun. Math. Phys. 146 (1992), 1–60, <http://projecteuclid.org/euclid.cmp/1104249974>.
- [12] A.G. Izergin, D.A. Coker and V.E. Korepin, *Determinant formula for the six-vertex model*, J. Phys. A 25 (1992), 4315.
- [13] B. Derrida, M. Evans, V. Hakim and V. Pasquier, *Exact solution of a 1D asymmetric exclusion model using a matrix formulation*, J. Phys. A 26 (1993), 1493–1517.
- [14] G. Schutz and E. Domany, *Phase Transitions in an Exactly Soluble One-Dimensional Exclusion Process*, J. Stat. Phys. 72 (1993), 277, [arXiv:cond-mat/9303038](https://arxiv.org/abs/cond-mat/9303038).
- [15] G.E. Andrews, *Plane partitions V: the TSSCPP conjecture*, J. Combin. Theory A 66 (1994), 28–39.
- [16] F. Essler and V. Rittenberg, *Representations of the quadratic algebra and partially asymmetric diffusion with open boundaries*, J. Phys. A 29 (1996), 3375–3407, [arXiv:cond-mat/9506131](https://arxiv.org/abs/cond-mat/9506131).
- [17] D. Zeilberger, *Proof of the alternating sign matrix conjecture*, Electron. J. Combin. 3(2) (1996), R13, [arXiv:math/9407211](https://arxiv.org/abs/math/9407211).
- [18] L.D. Faddeev, *How Algebraic Bethe Ansatz works for integrable model*, Les Houches lecture notes (1995), [arXiv:hep-th/9605187](https://arxiv.org/abs/hep-th/9605187).
- [19] B. Derrida, *An exactly soluble non-equilibrium system: the asymmetric simple exclusion process*, Physics Reports 301 (1998), 65–83.
- [20] A.I. Molev and B.E. Sagan, *A Littlewood–Richardson rule for factorial Schur functions*, Transactions of the American Mathematical Society 351(11) (1999), 4429–4443, [arXiv:q-alg/9707028](https://arxiv.org/abs/q-alg/9707028).
- [21] G. Kuperberg, *Another proof of the alternating sign matrix conjecture*, Int. Math. Research Notes (1996) 139–150, [arXiv:math/9712207](https://arxiv.org/abs/math/9712207).
- [22] H. Cohn, M. Larsen, J. Propp, *The shape of a typical boxed plane partition*, New York Journal of Mathematics 4 (1998), 137–165, [arXiv:math/9801059](https://arxiv.org/abs/math/9801059).
- [23] W. Jockush, J. Propp, P. Shor, *Random Domino Tilings and the Arctic Circle Theorem*, [arXiv:math.CO/9801068](https://arxiv.org/abs/math.CO/9801068).
- [24] D. Bressoud, *Proofs and confirmations: The story of the alternating sign matrix conjecture*, Mathematical Association of America (1999).
- [25] A. Kirillov Jr and A. Lascoux, *Factorization of Kazhdan–Lusztig elements for Grassmanians*, Adv. Stud. 28 (2000), 143–143, [arXiv:math.CO/9902072](https://arxiv.org/abs/math.CO/9902072).
- [26] V. Korepin, P. Zinn-Justin, *Thermodynamic limit of the six-vertex model with domain wall boundary conditions*, J. Phys. A 33 (2000), 7053–7066, [arXiv:cond-mat/0004250](https://arxiv.org/abs/cond-mat/0004250).
- [27] P. Zinn-Justin, *Six-vertex model with domain wall boundary conditions and one-matrix model*, Phys. Rev. E (3) (2000), 3411–3418, [arXiv:math-ph/0005008](https://arxiv.org/abs/math-ph/0005008).
- [28] A. V. Razumov and Yu. G. Stroganov, *Spin chain and combinatorics*, J. Phys. A 34 (2001), 3185–3190, [arXiv:cond-mat/0012141](https://arxiv.org/abs/cond-mat/0012141).
- [29] A. Lascoux, *Symmetric functions and combinatorial operators on polynomials*, CBMS 99, American Mathematical Society (2001).

- [30] M. T. Batchelor, J. de Gier and B. Nienhuis, *The quantum symmetric XXZ chain at $\Delta = -1/2$, alternating sign matrices and plane partitions*, J. Phys. A 34 (2001), L265–L270, [arXiv:cond-mat/0101385](#).
- [31] A. V. Razumov and Yu. G. Stroganov, *Spin chains and combinatorics: twisted boundary conditions*, J. Phys. A 34 (2001), 5335–5340, [arXiv:cond-mat/0102247](#).
- [32] A.V. Razumov and Yu.G. Stroganov, *Combinatorial nature of ground state vector of $O(1)$ loop model*, Theor. Math. Phys. 138 (2004), 333–337, [arXiv:math.CO/0104216](#).
- [33] A. Okounkov, N. Reshetikhin, *Correlation function of Schur process with application to local geometry of a random 3-dimensional Young diagram*, Amer. Math. Soc. 16 (2003), 581–603, [arXiv:math.CO/0107056](#).
- [34] Yu. Stroganov, *A New Way to Deal with Izergin-Korepin Determinant at a third Root of Unity*, Teor. Mat. Fiz. 1 (2006), 65–76, [arXiv:math-ph/0204042](#).
- [35] P. Zinn-Justin, *The Influence of Boundary Conditions in the Six-Vortex Model*, unpublished, [arXiv:cond-mat/0205192](#).
- [36] J. de Gier, *Loops, matchings and alternating-sign matrices*, Discr. Math. 298 (2005), 365–388; [arXiv:math.CO/0211285](#).
- [37] A. Okounkov, N. Reshetikhin, C. Vafa, *Quantum Calabi–Yau and Classical Crystals*, [arXiv:hep-th/0309208](#).
- [38] S. Okada, *Enumeration of symmetry classes of alternating sign matrices and characters of classical groups*, J. Algebraic Combin. 23 (2006), 43–69, [arXiv:math/0408234](#).
- [39] P. Di Francesco, P. Zinn-Justin and J.-B. Zuber, *Determinant formulae for some tiling problems and application to fully packed loops*, Ann. Inst. Fourier (Grenoble) 55(6) (2005), 2025–2050, [arXiv:math-ph/0410002](#).
- [40] P. Di Francesco and P. Zinn-Justin, *Around the Razumov–Stroganov conjecture: proof of a multi-parameter sum rule*, Electron. J. Combin. 12 (2005) R6, [arXiv:math-ph/0410061](#).
- [41] K. Johansson, *The arctic circle boundary and the Airy process*, Ann. Probab. 33 (2005), 1–30.
- [42] D. Allison and N. Reshetikhin, *Numerical study of the 6-vertex model with Domain Wall Boundary Conditions*, [arXiv:cond-mat/0502314](#).
- [43] V. Pasquier, *Quantum incompressibility and Razumov Stroganov type conjectures*, Ann. Henri Poincaré 7 (2006), 397–421, [arXiv:cond-mat/0506075](#).
- [44] P. Di Francesco and P. Zinn-Justin, *Quantum Knizhnik–Zamolodchikov equation, generalized Razumov–Stroganov sum rules and extended Joseph polynomials*, J. Phys. A 38 (2005), L815–L822, [arXiv:math-ph/0508059](#).
- [45] K. Johansson, *Random matrices and determinantal processes*, Les Houches lectures, [arXiv:math-ph/0510038](#).
- [46] V. Pasquier, *Incompressible representations of the Birman–Wenzl–Murakami algebra*, [arXiv:math/0507364](#).
- [47] P. Bleher, V. Fokin, *Exact Solution of the Six-Vortex Model with Domain Wall Boundary Conditions. Disordered Phase*, Commun. Math. Phys. 268 (2006), 223–284. [arXiv:math-ph/0510033](#).
- [48] P. Di Francesco, P. Zinn-Justin, J.-B. Zuber, *Sum rules for the ground states of the $O(1)$ loop model on a cylinder and the XXZ spin chain*, J. Stat. Mech. (2006) P08011, [arXiv:math-ph/0603009](#).
- [49] P. Zinn-Justin, *Proof of the Razumov–Stroganov conjecture for some infinite families of link patterns*, Electron. J. Combin. 13(1) (2006), R110, [arXiv:math/0607183](#).
- [50] P. Di Francesco, *Totally Symmetric Self-Complementary Plane Partitions and Quantum Knizhnik–Zamolodchikov equation: a conjecture*, J. Stat. Mech. (2006) P09008, [arXiv:cond-mat/0607499](#).
- [51] P. Di Francesco and P. Zinn-Justin, *Quantum Knizhnik–Zamolodchikov Equation, Totally Symmetric Self-Complementary Plane Partitions and Alternating Sign Matrices*, Theor. Math. Phys. 154(3) (2008), 331–348, [arXiv:math-ph/0703015](#).
- [52] F. Colomo, A.G. Pronko, *The Arctic Circle Revisited*, [arXiv:0704.0362](#).
- [53] A.V. Razumov, Yu.G. Stroganov and P. Zinn-Justin, *Polynomial solutions of qKZ equation and ground state of XXZ spin chain at $\Delta = -1/2$* , J. Phys. A 40 (39) (2007), 11827–11847, [arXiv:0704.3542](#).
- [54] J.W. van de Leur, A.Yu. Orlov, *Random turn walk on a half line with creation of particles at the origin*, [arXiv:0704.1157](#).
- [55] F. Colomo, A.G. Pronko, *Emptiness formation probability in the domain-wall six-vertex model*, [arXiv:0712.1524](#).

- [56] J. de Gier, P. Pyatov, *Factorised solutions of Temperley–Lieb q KZ equations on a segment*, arXiv:0710.5362.
- [57] P. Bleher, K. Liechty, *Exact Solution of the Six-Vertex Model with Domain Wall Boundary Conditions. Ferroelectric phase*, arXiv:0712.4091.
- [58] D. Zeilberger, *Proof of a Conjecture of Philippe Di Francesco and Paul Zinn-Justin Related to the q KZ Equations and to Dave Robbins’ Two Favorite Combinatorial Objects*, <http://www.math.rutgers.edu/~zeilberg/mamarim/mamarimhtml/diFrancesco.html>, 2007.
- [59] J. Harnad, A.Yu. Orlov, *Fermionic construction of tau functions and random processes*, arXiv:0801.0066.
- [60] P. Bleher, K. Liechty, *Exact Solution of the Six-Vertex Model with Domain Wall Boundary Conditions. Critical line between ferroelectric and disordered phases*, arXiv:0802.0690.
- [61] T. Fonseca and P. Zinn-Justin, *On the Doubly Refined Enumeration of Alternating Sign Matrices and Totally Symmetric Self-Complementary Plane Partitions*, to appear in *Electron. J. Combin.*, arXiv:0803.1595.
- [62] F. Colomo, A.G. Pronko, *The limit shape of large alternating sign matrices*, arXiv:0803.2697.

PAUL ZINN-JUSTIN, LPTMS (CNRS, UMR 8626), UNIV PARIS-SUD, 91405 ORSAY CEDEX, FRANCE;
 AND LPTHE (CNRS, UMR 7589), UNIV PIERRE ET MARIE CURIE-PARIS6, 75252 PARIS CEDEX,
 FRANCE.

E-mail address: pzinn@lpthe.jussieu.fr